Published in Cretaceous Research 28, issue 6, 939-960, 2007
which should be used for any reference to this work

High stress late Maastrichtian – early Danian palaeoenvironment in the Neuquén Basin, Argentina

G. Keller [a,*], T. Adatte [b], A.A. Tantawy [c], Z. Berner [d], W. Stinnesbeck [e], D. Stueben [d], H.A. Leanza [f]

[a] *Department of Geosciences, Princeton University, Princeton, NJ 08540, USA*
[b] *Geological Institute, University of Neuchatel, Neuchatel CH-2007, Switzerland*
[c] *Department of Geology, South Valley University, Aswan, Egypt*
[d] *Institut für Mineralogie und Geochemie, Universität Karlsruhe, 76128 Karlsruhe, Germany*
[e] *Geologisch-Paläontologisches Institut, Universität Heidelberg, Neuenheimer Feld 234, 69120 Heidelberg, Germany*
[f] *Servicio Geologico Minero Argentino y CONICET, 1067 Buenos Aires, Argentina*

Abstract

During the late Maastrichtian to early Danian the Neuquén Basin of Argentina was adjacent to an active volcanic arc to the west and an extensive land area to the northeast. Mineralogical and geochemical studies of the Bajada del Jagüel in the Neuquén Basin indicate a generally warm climate with seasonal changes in humidity and an open seaway to the South Atlantic that maintained marine conditions. Biostratigraphic and quantitative foraminiferal and nannofossil analyses indicate that sediment deposition during the late Maastrichtian (zones CF4-CF2, *N. frequens*) occurred in relatively shallow middle neritic (~100 m) depths with largely dysaerobic bottom waters (abundant low O_2 tolerant benthics) and fluctuating sea level. Calcareous nannofossils indicate a high stress marine environment dominated by *Micula decussata.* Planktic foraminifera mimic the post-K/T high stress environment with alternating blooms of the disaster opportunists *Guembelitria* and low oxygen tolerant *Heterohelix* groups, indicating nutrient-rich surface waters and an oxygen depleted water column. The high stress conditions were probably driven by high nutrient influx due to upwelling and terrestrial and volcanic influx. The K/T boundary is marked by an erosional surface that marks a hiatus at the base of a 15-25 cm thick volcaniclastic sandstone, which contains diverse planktic foraminiferal zone P1c assemblages and nannofossils of zone NP1b immediately above it. This indicates deposition of the sandstone occurred ~500 ky after the K/T hiatus. No evidence of the Chicxulub impact or related tsunami deposition was detected.

Keywords: Argentina; Maastrichtian; K/T; Paleoenvironment

1. Introduction

Over the past 15 years, land-based marine sections have yielded far more continuous and high sedimentation records of the end-Cretaceous mass extinction than any deep-sea cores with their condensed and often discontinuous records. Much of our current understanding of the end-Cretaceous mass extinction, impacts, and environmental changes has come from intensive studies of land-based marine sequences from Central America, the southern United States, eastern and western Tethys and northern high latitudes. Two stories have emerged from these records. (1) The biotic effects of the mass extinction were highly variable among different fossil groups. Planktic foraminifera were the clear loosers with all tropical and subtropical species (2/3 of all species) extinct coincident with the deposition of a global iridium anomaly that marks a major impact. All but a few survivors died out during the first 200-300 ky of the Danian. Calcareous nannoplankton suffered strong declines, but some thrived well into the Tertiary. All other microfossil groups reveal lesser biotic effects (Keller, 2001; MacLeod, 1998; Paul, 2005; Twitchett, 2006). (2) There were two major impacts. The Cretaceous/Tertiary (K/T) boundary

* Corresponding author.
E-mail address: gkeller@princeton.edu (G. Keller).

impact is recognized by the global iridium anomaly and frequently Ni-rich spinels. The Chicxulub impact is recognized by glass spherule ejecta, and predates the K/T boundary by ~300 ky as indicated by the spherule ejecta interbedded in late Maastrichtian sediments in northeastern Mexico and Texas (review in Keller et al., 2003, 2007) and the impact breccia below the K/T boundary in the Chicxulub crater core Yaxcopoil-1 (Keller et al., 2004a,b). No iridium enrichment has ever been documented in association with Chicxulub impact ejecta in marine sediments with continuous sediment accumulation. Reports of the juxtaposition of the Ir anomaly with a thin impact spherule layer on Blake Nose off Florida (Norris et al., 1999) and Demerara Rise, southwestern North Atlantic (MacLeod et al., 2007) show undulating erosional surfaces at the base and top of a 1-3.5 cm thin spherule layer with reworked foraminifera. This suggests erosion and redeposition of the spherules from older deposits, similar to the thick reworked spherule deposits at the base of sandstone deposits found throughout NE Mexico, where the original spherule deposit is 4-5 m below and interbedded in undisturbed marine marls of late Maastrichtian age near the base of zone CF1.

Although these Chicxulub impact findings have been documented in dozens of sequences in Mexico, Belize and Guatemala, the global distribution and the biotic effects of the Chicxulub impact are still unknown. Most of all, the K/T transition in South America is poorly known largely due to a lack of outcrops, diagenetic alteration, or very shallow depositional environments. However, K/T outcrops have been reported from Pernambuco in NE Brazil (Albertão et al., 1994; Albertão and Martins, 1996; Stinnesbeck and Keller, 1996; Marini et al., 1998; Martins et al., 1998).

In Argentina, the Neuquén Basin has the best exposures of Upper Cretaceous to lower Paleogene rocks and this has led us to investigate these sequences in order to evaluate the K/T impact hypothesis and Chicxulub impact ejecta layer in particular. During the Maastrichtian, the Neuquén Basin was flooded by an extensive sea that connected the basin to the South Atlantic and reached the area of the present Andes to the west (Fig. 1). In the southeastern part, marine environments persisted into the Paleocene. Towards the west contemporaneous volcanic activity led to emergence in the area of the present Andes, which separated the Neuquén Basin from the Pacific (Fig. 1) (Uliana and Biddle, 1988). The Bajada del Jagüel section in the Neuquén Basin has reportedly the best K/T record and was first studied by Bertels (1970, 1980, 1987) based on ostracods and foraminifer. Subsequently, other workers documented calcareous nannofossils, dinoflagellates, palynomorphs, planktic and benthic foraminifera and sedimentary environments with sometime contradictory results (Casadío, 1994, 1998; Nañez and Concheyro, 1997; Papú et al., 1999; Scasso et al., 2005).

In this study we report on the upper Maastrichtian to lower Paleocene sequence of the Bajada del Jagüel section in the Neuquén Basin. The primary objectives are to evaluate the continuity of the sedimentary record, the depositional environment, biotic stress and sea level changes during the late Maastrichtian

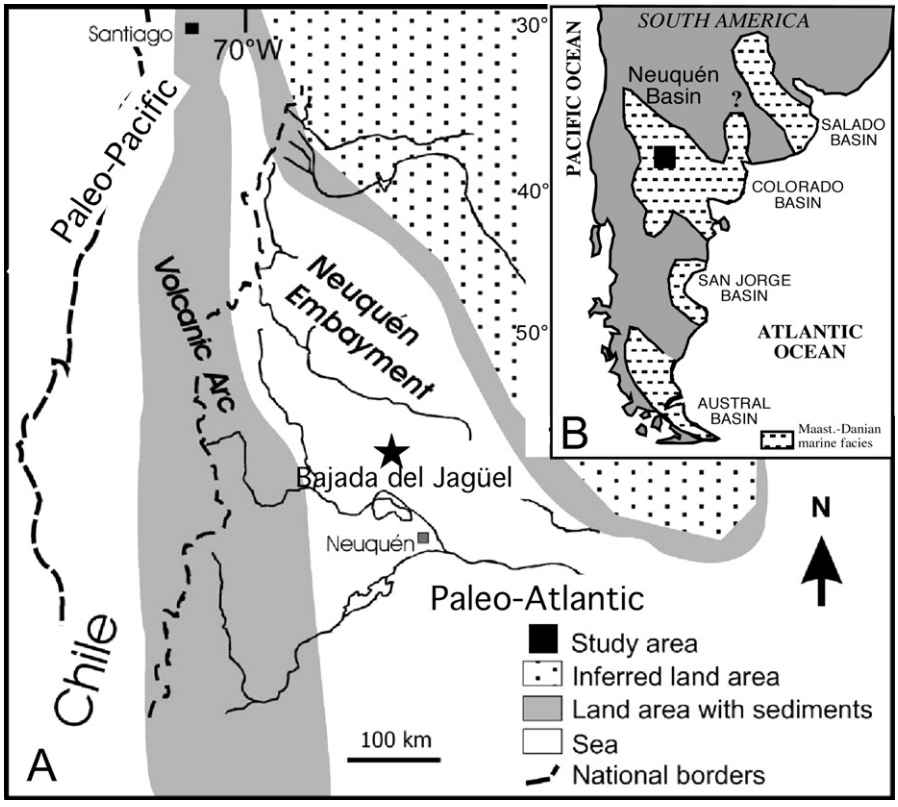

Fig. 1. A, Palaeogeographic map of the Neuquén Basin, the volcanic arc and the Bajada del Jagüel section in Argentina (modified after Scasso et al., 2005). B, Geographic map of South America showing the marine incursion during the Maastrichtian and early Paleocene.

to early Danian. Analytical methods include quantitative microfossil analyses (planktic foraminifera and calcareous nannofossils), stable isotopes, whole rock and clay mineralogy and total organic content.

2. Methods and material

The Bajada del Jagüel section was measured and examined for lithological changes, macrofossils, trace fossils, bioturbation, erosion surfaces and hardgrounds. A total of 120 samples were analyzed for microfossils, mineralogy and geochemistry. The section was collected at 50 cm intervals for the first 16 m of the Maastrichtian, followed by 20-25 cm spacing for the next 13 m up to 3.5 m above the K/T unconformity and at 50 cm for the next 10 m of the Danian. Several additional outcrops were sampled in the Neuquén Basin (e.g., Lomas Coloradas, General Roca, Huantraico, Fig. 1), though these were found to have only rare or poorly preserved microfossils, except for the General Roca section, which exposes the same Danian stratigraphic sequence as the Bajada del Jagüel section.

Samples were processed for planktic and benthic foraminifera by standard methods (Keller, 2002). Planktic foraminifera were analyzed quantitatively from the >63 μm size fraction based on representative sample splits with 100 to 250 specimens for the Maastrichtian through the first 3.5 m of the Danian. Benthic foraminifera in the sample split were counted to obtain the benthic/planktic ratio. The remaining sample residue was examined for rare species, the presence of macrofossils, volcanic sediments and pyrite. The fine fraction (>38 μm) was examined for the presence of dwarfed species. Planktic foraminifera are generally well preserved. Calcareous nannofossils were processed by standard smear slide preparation and quantitatively examined based on the procedure of Jiang and Gartner (1986), Pospichal (1991) and Tantawy (2003a,b). All sample material, including the washed residues and picked slides are curated in the Micropaleontology collection of Princeton University.

For geochemical and mineralogical analyses, samples were dried, crushed, finely ground in an agate mill, and dried at 105 °C. Clay mineral analyses were conducted at the Geological Institute of the University of Neuchatel, Switzerland, based on XRD analyses (SCINTAG XRD 2000 Diffractometer). Sample processing followed the procedure outlined by Kübler (1987) and Adatte et al. (1996). The origin and amount of organic matter were determined by Rock-Eval pyrolysis using a Rock-Eval 6 (Behar et al., 2001) at the Geological Institute of the University of Neuchâtel, Switzerland. Standard notations are used: total organic carbon (TOC) content in weight %; hydrogen index ($HI = S_2/TOC \times 100$) in mg hydrocarbons per g of TOC; oxygen index ($OI = S_3/TOC \times 100$) in mg CO2 per g of TOC.

Stable carbon and oxygen isotope data were obtained from bulk rock samples at the Institute for Mineralogy and Geochemistry at Karlsruhe using a fully automated preparation system (MultiCarb) connected on-line to an isotope ratio mass spectrometer (Optima, Micromass Limited UK). All carbon and oxygen isotope values are reported relative to V-PDB standard. Precision was better than 0.06‰ for $\delta^{13}C$ and <0.1‰ for $\delta^{18}O$.

3. Location and lithology

Cretaceous-Tertiary (K/T) outcrops are exposed throughout the Neuquén Basin, but the classical boundary locality is the Bajada del Jagüel section located in the Neuquén Province about 500 m east of provincial road #8 on the western side of a meseta (38° 06′ 25″ S, 68° 23′ 36″ W). More than 30 m of upper Maastrichtian to Danian mudstone of the Jagüel Formation is exposed, followed by over 10 m of marly limestone of the Paleocene Roca Formation (Bertels, 1979; Uliana and Dellapié, 1981; Legarreta and Gulisano, 1989) (Fig. 2). The Jagüel Formation studied in this report spans the interval between the evaporite bed at the top of the Allen Formation below and the first limestone of the Roca Formation at the top. The base of the Roca Formation is time transgressive and assigned to the Maastrichtian in the northwest of the Neuquén Basin and to the Danian in the center and south (Bertels, 1964, 1970; Casadío, 1994).

The Jagüel Formation forms the lower 2/3 of the hill flank with the Roca Formation the upper 1/3 to the top (Fig. 2). Bedding is almost horizontal with no apparent tectonic disturbance. About 40 m was sampled encompassing the upper part of the Jagüel Formation up to the contact with the overlying Roca Formation. The lower 17 m of the section consist of grey-green friable claystone with abundant diagenetic gypsum veins and rare oysters. In the upper part, the silt content gradually increases. An erosional surface marks the contact between the claystone and overlying marl at 17 m. The two marl beds between 17 m and 18.5 m contain rare bivalves (e.g., *Pycnodonte (Phygraea) vesicularis* (Lamarck) and *Chlamys* sp.) and internal moulds of gastropods. Volcanic-rich siltstone beds are identified at 9.5 m, l9.8 m, 22.5 m and 27-28 m. *Chondrites* is the only trace fossil identified and pyrite framboids are common.

At about 25 m from the base of the section, there is a 25 cm thick grey marly limestone with an erosional surface at the top. Above it there is a 15-25 cm thick yellow sandstone rich in diagenetic gypsum and volcanic debris, such as idiomorphic plagioclase of volcanic origin and devitrified glass (e.g. tuffite, Fig. 3). Above the volcanic-rich sandstone is a 20 cm thick dark grey silty claystone, followed by grey siltstone and a volcanic-rich silty claystone (27-28 m). Above this interval, grey silty marlstone beds (10-20 cm thick) contain bivalves (oysters, pectinids), gastropods and occasional echinoids. This marlstone sequence is 12 m thick and abruptly terminates at the top by the overlying 15 m thick sequence of grey limestones with pycnodontid oysters of the Roca Formation.

4. Biostratigraphy

4.1. Maastrichtian

4.1.1. Calcareous nannofossils

The biozonation used in this paper is based on Sissingh (1977), Perch-Nielsen (1981a,b) and modified by Tantawy

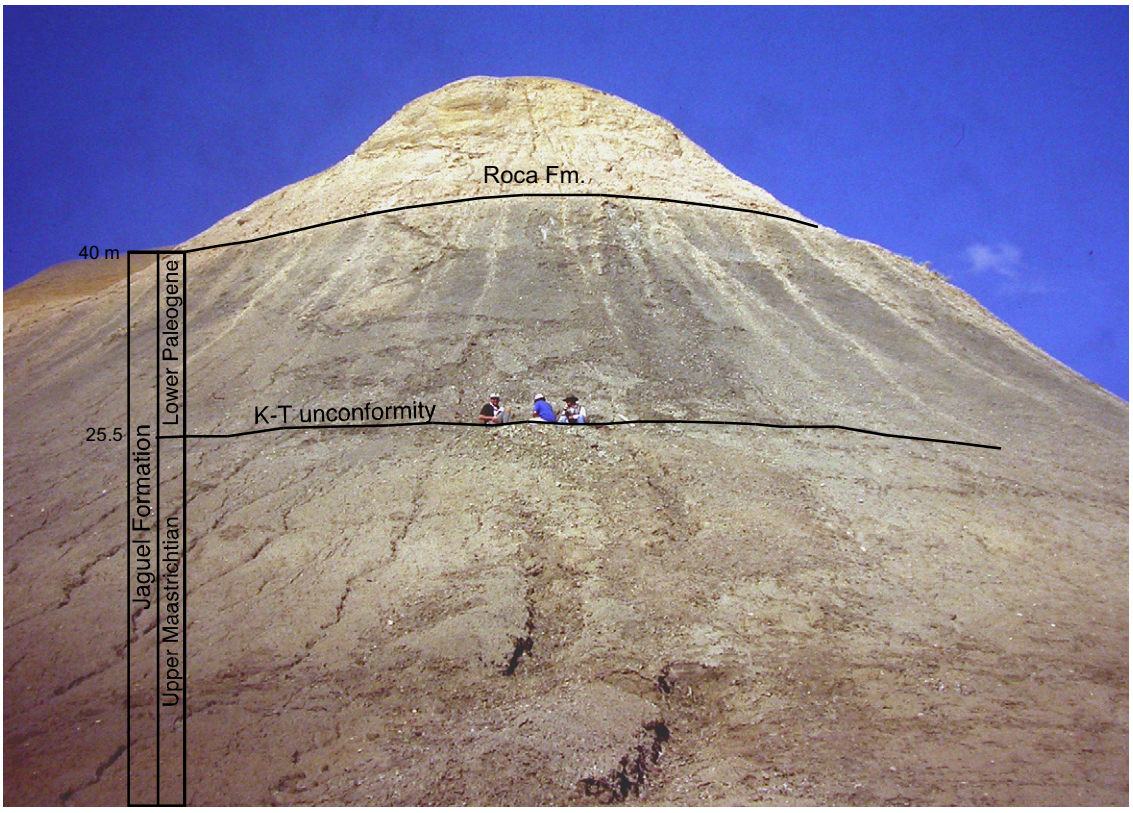

Fig. 2. Photo of the Bajada del Jagüel outcrop showing exposures of the Jagüel and Roca formations and the Cretaceous/Tertiary unconformity.

Fig. 3. The Cretaceous/Tertiary unconformity in the Jagüel section. The yellow volcaniclastic sandstone overlies the undulating erosional surface that marks the K/T unconformity. Arrows point to rip-up clasts of the underlying claystone.

(2003a,b), Tantawy and Keller (2004) as shown in Fig. 4 with comparison with other biozonal schemes. The lower 25.5 m of the section are characteristic of the late Maastrichtian *Nephrolithus frequens* or zone CC26 (Fig. 5, Table 1). Throughout this interval *Micula decussatta* dominates, averaging 76% and reaching a maximum of 92%. In intervals of lower *M. decussata* abundances, *Prediscosphaera stoveri*, *Arkhangelskiella cymbiformis* and *Eiffellithus turriseiffelii* are common. All other species, including *N. frequens*, are minor components of the assemblages. In middle latitudes, the *N. frequens* zone spans all or most of the late Maastrichtian (including *Micula murus* and *M. prinsii* zones) and generally corresponds to planktic foraminiferal zones CF1-CF3 (Fig. 4). However, *N. frequens* is time transgressive and appears earlier in southern high latitudes (Pospichal and Wise, 1990), as also observed in the Bajada del Jagüel section.

The absence of *M. prinsii* may be due to a hiatus, as suggested by the erosional unconformity that marks the top of the grey marly limestone, or ecological exclusion. *Micula prinsii* tends to prefer low to middle latitudes, but is also commonly reported from middle to high latitudes, including DSDP Sites 216 (40°S) and 524 (45°S at similar latitudes as the Jagüel section, and from Denmark (50°N) (Perch-Nielsen et al., 1982; Tantawy and Keller, 2004). The absence of *M. prinsii* in the Jagüel section is thus likely due to a hiatus, as also observed at DSDP sites 761 and 762 (Pospichal and Bralower, 1992; Bralower and Siesser, 1992). The presence of only rare *Prediscosphaera stoveri* in the Jagüel section, except for two peaks of 20-30%, also suggests the removal of the uppermost Maastrichtian (Fig. 5). In the high southern latitudes (Sites 690, 738), *P. stoveri* dominates the assemblages with up to 70% directly below the K/T boundary (Pospichal and Wise, 1990; Wei and Thierstein, 1991), decreased to ~30% in middle latitudes (Site 752, 30° S Pospichal, 1991) and to 8% in lower latitudes (Site 761, 16° 44′ S, Pospichal and Bralower, 1992). The absence of an interval containing notably higher percentages of *P. stoveri* in the uppermost Maastrichtian of the Jagüel section therefore indicates a hiatus.

4.1.2. Planktic foraminifera

The biozonation of Li and Keller (1998a) and Keller et al. (1995) is used for the Maastrichtian and Danian (Fig. 4). Maastrichtian planktic foraminiferal assemblages are of very low diversity with 7 species commonly present, but reaching

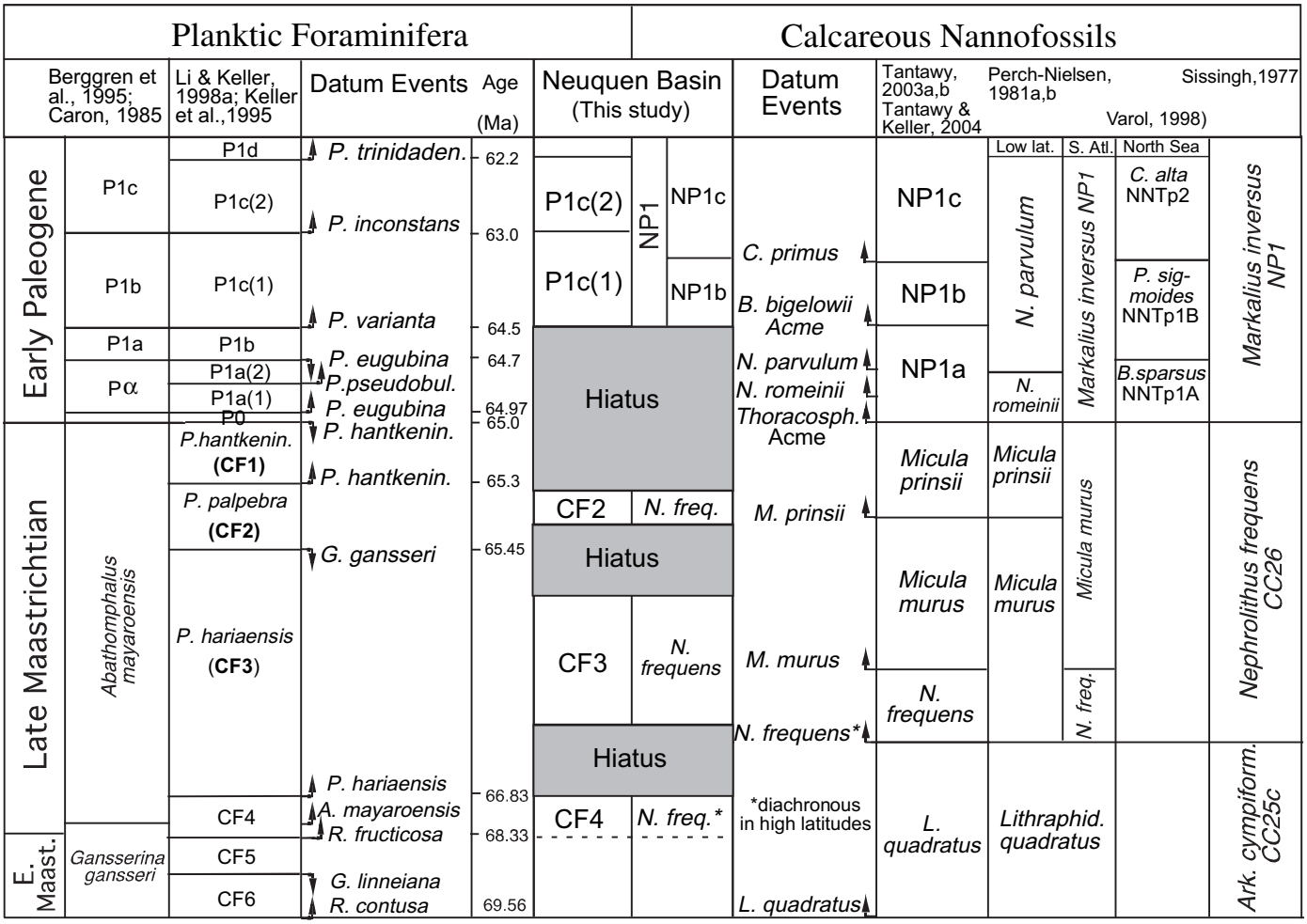

Fig. 4. Biozonations used in this study and comparison with other commonly used zonal schemes. Hiatuses in the Jagüel section inferred from biostratigraphy and sea level changes based on benthic foraminifera, microfossil assemblages, and the global sea level record. (Sources: Berggren et al., 1995; Caron, 1985; Li and Keller, 1998a; Keller et al.,1995; Tantawy, 2003a,b; Tantawy and Keller, 2004; Perch-Nielsen, 1981a,b; Sissingh,1977; Varol, 1998.)

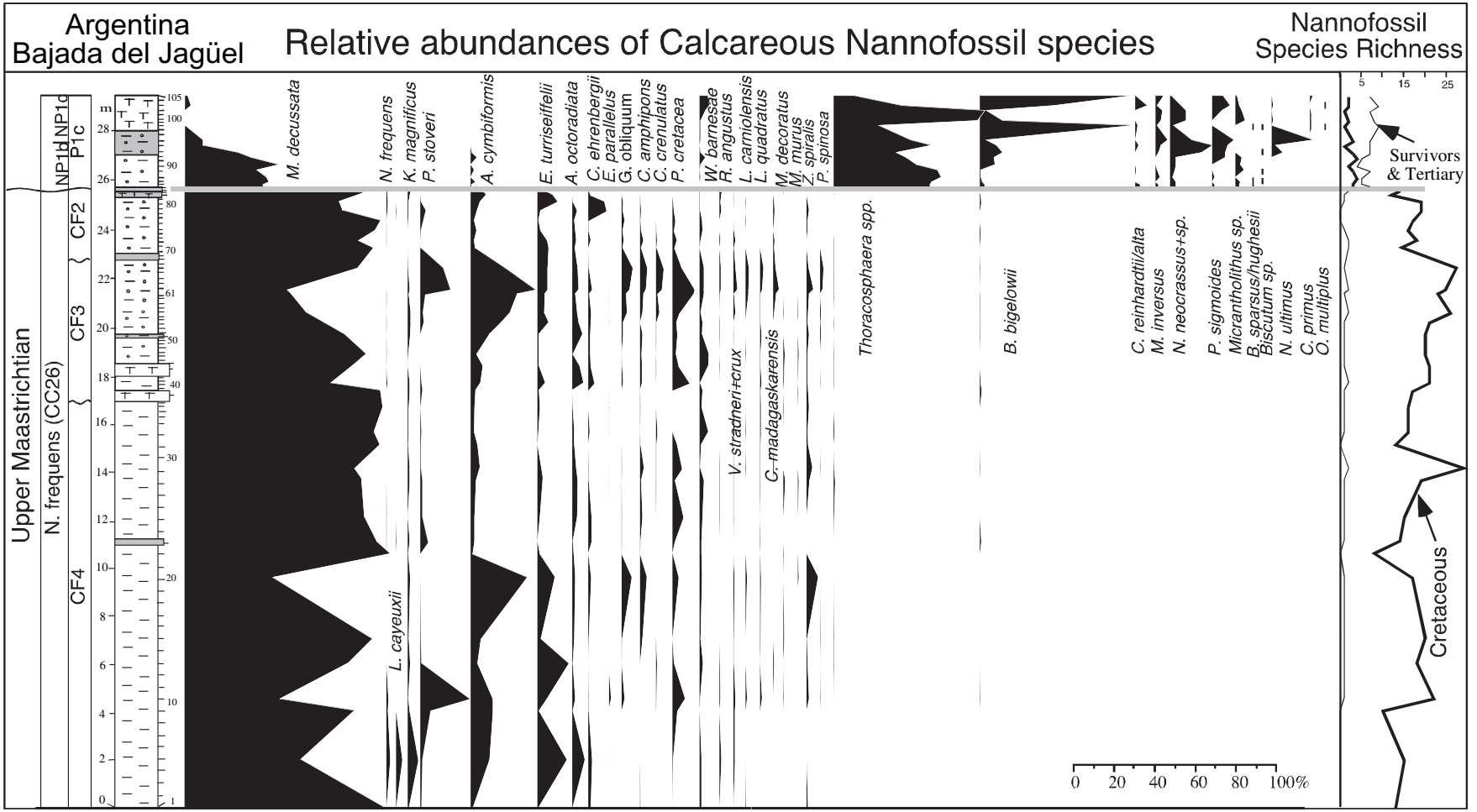

Fig. 5. Relative abundance of calcareous nannofossils in the Jagüel section. Note the dominance of *Micula decussata* throughout the late Maastrichtian marks high-stress conditions. The sudden appearance of *Throacosphaera* blooms and Tertiary species above the volcaniclastic sandstone mark zone NP1b with the early Danian NP1a missing. See legend for lithology on Fig. 6.

Table 1
Relative species abundances of calcareous nannofossils in the upper Maastrichtian and lower Paleocene of the Jagüel section of the Neuquén Basin, Argentina

Cretaceous species

Age	Zone	Zone	Sample No.	Total counted	*Ahmuellerella octoradiata*	*Arkhangelskiella cymbiformis*	*Chiastozygus amphipons*	*Corollithion? madagaskarensis*	*Cretarhabdus crenulatus*	*Cribrosphaerella ehrenbergii*	*Dodekapodorhabdus noeliae*	*Eiffellithus gorkae*	*Eiffellithus parallelus*	*Eiffellithus turriseiffelii*
Danian	NP1	NNTp2	105	268										
			103	264										
			102	126										
			100	298						2				
			98	364										
			95	262										2
		NNTp1B	94	228										
			93	304		2								
			92	62		2				2				2
			90	280										
			89	224		4								2
			88	328								2		2
			87	404		10				2				
			86	342		2								4
			84-85	Barren										
Late Maastrichtian	*Nephrolithus frequens* (CC26)		83	354		22				1		3		15
			82	371		27				4		2		26
			80	489	2	21	1	1		36		9		46
			78	407	10	12	2	3		35		10	1	5
			76	329	3	6	X	2		X		3	X	1
			74	339	5	9	2		1	1		4		4
			72	369	7	6	6	2	2	4		6		16
			70	342	4	7	2	X	1	1		3		17
			65	612	9	69	17	1	20	1		8	1	18
			60	426	6	90	9	5	9	2	1	6	2	15
			59	404	6	88	6	5	3	2		2	2	13
			55	379	9	70	4	1	6	5		11	1	12
			53	461	14	66			1	5		10	2	24
			50	470	23	42	6		1	4		3		3
			45	408	1	12	3			4		1		3
			43	382	13	22	3	1	1	4		1		2
			41	371	20	17	3			11		3		13
			38	361		9						1	1	2
			35	539	2	10	X					X	3	6
			32	278	3	5			2	2			X	X
			31	309	3	10	1		1					
			29	334	11	20	6	1	1	X	1	1	1	6
			28	385	10	10	2		1	1			2	15
			25	482	11	9	5			7		2		5
			23	310	1	6	1			5				
			22	314	2	3						1		3
			20	284	4	78	9			4				23
			15	530	6	26	6		1	1				8
			13	421	1	13		1	2					61
			10	352	5	37			1	1		2	5	15
			9	316	1	33				1				2
			5	322	19	29				6		6	1	44
			1	534		6	1			6		3		1

Cretaceous species (continued)

Sample No.	*Gartnerago obliquum*	*Kamptnerius magnificus*	*Lithraphidites carniolensis*	*Lithraphidites quadratus*	*Lucianorhabdus cayeuxii*	*Microrhabdulus decoratus*	*Micula decussata*	*Micula murus*	*Nephrolithus frequens*	*Podorhabdus decorus*	*Prediscosphaera cretacea*	*Prediscosphaera mahajunga*	*Prediscosphaera grandis*	*Prediscosphaera stoveri*	*Prediscoaphaera spinosa*
105							4								
103							8								
102															
100															
98															
95							24								
94							20								
93							80								
92							20								
90							130								
89							80								
88							132								
87							166								
86							130								
84-85	Barren														
83		5				X	300		2						
82		3					300		2						
80	4	2	1		1		350		3		1			1	
78	2	2			1		300		2		3			10	
76	3	1	X				300				4			2	
74	2						300		1		2			1	
72	4						300		1		7				
70	2						300				3				
65	22	1	8	6			330				35			41	4
60	13	3	2	1			138			1	55	X		42	1
59	8	2	6	X			200		1		40			4	
55	10	5	1	X		1	215	1			12		1	4	2
53	4	6		X			300		1		8			7	1
50	4	6		3			350				10				2
45		X	1	1		3	350	2	X		6				
43	X			1		2	300	1		X	11	1			
41	3	3		2		1	253		2		30			2	1
38		3		X			330	1						3	
35		3		2		1	500		1						
32		X	X	1			250							1	
31		1		1			280				6			1	
29	X	4	X	X			250			X	15	2	1	1	1
28		9		1		3	305	2			4			3	
25	1						403		1		25			4	
23	1	3		1	1		260		1		3			22	
22		1				1	300								
20	15	3	2	1			116				8				
15	2	2		1		2	464		1					1	1
13		5					320				3			2	
10	5	1	3	3		1	156		4		20			81	1
9		3					250		2		7			15	
5		16			10		174		6		X			3	
1		3	2				500							3	

Cretaceous species (continued) and Survivors + Tertiary species

Sample No.	*Rhagodiscus angustus*	*Vekshinella crux*	*Vekshinella stradneri*	*Watznaueria barnesae*	*Zygodiscus spiralis*	*Zygodiscus pseudoanthophorus*	*Biscutum* sp	*Biantholithus sparsus*	*Biantholithus hughesii*	*Braarudosphaera bigelowii*	*Chiphramalithus ultimus*	*Cruciplacolithus primus*	*Cyclagelosphaera reinhardtii/alta*	*Markalius inversus*	*Micrantholithus* sp.	*Neocrepidolithus neocrassus/cruciatus*	*Octolithus multiplus*	*Placozygus sigmoides*	*Thoracosphaera* spp.
105				12						194		4		10	2	2		14	26
103				12						90	2		16	2	4	14	4	24	88
102				4						4				4	4	10		6	94
100				2						32	2	2		8	14	24			212
98				2			2	2		262	0	2	4	2		6	2		80
95				2						8	54	2	0	14		28		28	100
94				0						18	4		4	6		48		18	110
93				2			8			32	16		0	4		48		20	92
92				2						4	0		0	0	2	2		4	22
90				2						20	0		0	0	6	8			114
89				0			2			2	0		2	2	10	6			114
88				2						2				6		4		4	174
87							4		2	4				0	10	12			194
86									6	8			8	4	6	10		4	160
84-85	Barren																		
83	4		X	X						1									1
82	3	1		1						2									
80	2		1	1	2					4									
78	4			1	4														
76				2	1									1					
74			1	3	1					2									
72	2		3	2						X									1
70	X		1							X									1
65	3	1	3	9	1					2				1					1
60	1		4	7	7					3									3
59	1		1	8	4					1									1
55		1	2	2	2					1									
53	1			7	1					2									1
50	1		1	5	5					1				X					
45				18	1	1													1
43	1			16	1														1
41			2	1	1					2									1
38				5	2					4									
35			1	5	5					X									
32			1	12	X									X					1
31				2	2	1													
29	1		X	1	9					X				X					1
28	1	1		8	5														2
25	X		1	7															1
23				3						2									
22				3															
20			1	3	15	1							1						
15			1	3	1									2					1
13	1	1		7	2														1
10	2		3	1	4					1									
9			2																
5	3		2	3															
1				5	3									1					

13 species during a short interval marking an influx of temperate species (Fig. 6). All assemblages are dominated by *Guembelitria cretacea* and *G. dammula* (60-90%), variable abundances of *Heterohelix globulosa* (0-45%) and *H. dentata* (0-90%). *Pseudoguembelina costellifera*, *Zeauvigerina waiparaensis* and *Hedbergella* species are few to rare. The influx of temperate species between 11.3-13 m includes *Rugoglobigerina macrocephala*, *Globotruncana arca*, *G. aegyptiaca*, *Globigerinelloides aspera* and *Gansserina gansseri*, the latter species ranges from the base of the early Maastrichtian through zone CF3. Only one prominent global warm event occurred during this interval and it spanned from zone CF5 through the lower part of CF4 (Li and Keller, 1998a; Nordt et al., 2003; Abramovich and Keller, 2003). On this basis, the interval from 0-17 m that contains the influx of temperate species is tentatively assigned to zone CF4. An erosional contact between claystone and marlstone marks the top of this interval (Fig. 6).

Between 17 m and 22.8 m planktic foraminiferal assemblages are largely dominated by *Heterohelix dentata*, except for a short interval of >95% *Guembelitria* between 20-21 m. *Pseudoguembelina costellifera*, *H. globulosa*, *Zeauvigerina waiparaensis*, and rare *Hedbergella* and *Rugoglobigerina* are also present (Fig. 6, Table 2). A pronounced faunal change below the volcanic-rich silty claystone at 22.8 m is marked by the disappearance of five species and the onset of exclusive *Guembelitria* dominance. This abrupt faunal and lithological change suggests a hiatus with the dramatic drop in diversity likely associated with the global cooling and sea-level regression of 65.5 Ma that marks the CF3-CF2 transition. This global climatic change and regression is commonly recognized in continental shelf sequences in the US, Denmark, Tunisia, Egypt, Israel and Madagascar (Donovan et al., 1988; Schmitz et al., 1992; Keller et al., 1993; Li et al., 2000; Abramovich et al., 2002; Keller, 2002, 2004; Hart et al., 2005).

The uppermost part of the section from 22.8 m to the erosional contact between the marly limestone and volcaniclastic sandstone at 25.25 m is dominated exclusively by *Guembelitria*, except for minor *H. dentata* (<5%) near the base (Fig. 6). *Guembelitria*-dominated assemblages are well known from the post-K/T mass extinction and used to be considered indicative of earliest Danian age. However, these disaster opportunists thrived in any high-stress environments of the Cretaceous or Tertiary (Keller, 2002, 2003; Keller and Pardo, 2004), as also evident in the Jagüel section. The interval between 22.8-25.25 m is tentatively assigned to zone CF2. The uppermost Maastrichtian zone CF1 appears to be missing, as indicated by the absence of the index species and absence of influx of temperate species that should mark the prominent global warming of this biozone. The absence of the nannofossil *Micula prinsii* zone supports this age assignment.

4.2. K/T boundary

The K/T boundary is placed at 25.5 m marked by the erosional unconformity between the marly limestone with bivalves, echinoids, ostracods and the volcaniclastic sandstone and overlying gypsum-rich yellow volcanic-rich sandstone (Figs. 5, 6). This placement is consistent with the K/T boundary identified by earlier workers (e.g., Bertels, 1970, 1980; Nañez and Concheyro, 1997; Papú et al., 1999; Scasso et al., 2005). The first Danian planktic foraminifera are present in this sandstone and mark the abrupt appearance of seven species that characterize subzone P1c(1) (e.g., *Parasubbotina pseudobulloides*, *P. varianta*, *Parvularugoglobigerina extensa*, *Globoconusa daubjergensis*, *Eoglobigerina edita*, *Subbotina triloculinoides*, Fig. 6, Table 1). This indicates a hiatus with the early Danian zones P0, P1a and P1b missing, or about the first 500 ky of the Paleocene (Fig. 4). Olsson et al. (1999) note the extinction of *P. extensa* (formerly *G. conusa*) as marking the top of Pα or zone Pla in this study (Fig. 4). However, the presence of *P. extensa* in zone P1c in the Neuquén Basin, as well as the eastern Tethys, suggests that the range of this species may be diachronous.

No nannofossils were observed in the volcaniclastic sandstone. The zone NP1 index species *Biantholithus sparsus*, as well as *Cyclagelosphaera reinhardtii*/*alta*, *Placozygus sigmoides*, *Neocrepidolithus neocrassus*/*cruciatus* and the *Thoracosphaera sp.* acme first appear at the base of the claystone (sample 86) directly above it (Fig. 5). The first appearance of *P. sigmoides* marks the base of subzone NP1b (or NNTp1B of Varol, 1998, Fig. 4). This indicates that the earliest Danian zone NP1a is missing, consistent with the hiatus recognized based on planktic foraminifera.

4.3. Danian

In contrast to the Maastrichtian, Danian planktic foraminiferal assemblages are similar to those in middle and lower latitudes and can therefore be easily correlated with the global biostratigraphy. The Danian interval examined spans from the K/T boundary at 25.5 m to 40 m, marked by the base of the grey limestone that defines the base of the Roca Formation (Fig. 2). No planktic foraminifera or nannofossils were found in this limestone. In the 14.5 m below are Danian planktic foraminiferal assemblages characteristic of zone P1c. The lower 7.5 m of this interval contains diverse planktic foraminiferal assemblages indicative of Plc(1) with common *Praemurica taurica*, *Globoconusa daubjergensis*, *Parvularugoglobigerina extensa*, *Eoglobigerina edita* and few *Parasubbotina varianta*, *P. pseudobulloides*, *S. triloculinoides* and *S. trivialis* (Table 2, Fig. 6). The presence of *Praemurica inconstans* in the upper part suggests subzone P1c(2).

Nannofossil preservation varies from poor to good throughout the Danian. The first Danian assemblage indicates zone NP1b, dominated by Tertiary species and Cretaceous survivors, such as *Biantholithus sparsus*, *Neochiastozygus ultimus*, *Cyclagelosphaera reinhardtii*/*alta*, *Markalius inversus*, *Neocrepidolithus neocrassus*/*cruciatus*, *Thoracosphaera sp.*, *Braarudosphaera bigelowii* (Fig. 5, Table 1). Cretaceous reworked taxa are few to rare (e.g. *M. decussata*, *A. cymbiformis*, *W. barnesae*, *Eiffellithus turriseiffelii*, *Micrantholithus hoschulzii* and *M. obtusus*). *Cruciplacolithus primus* first occurs

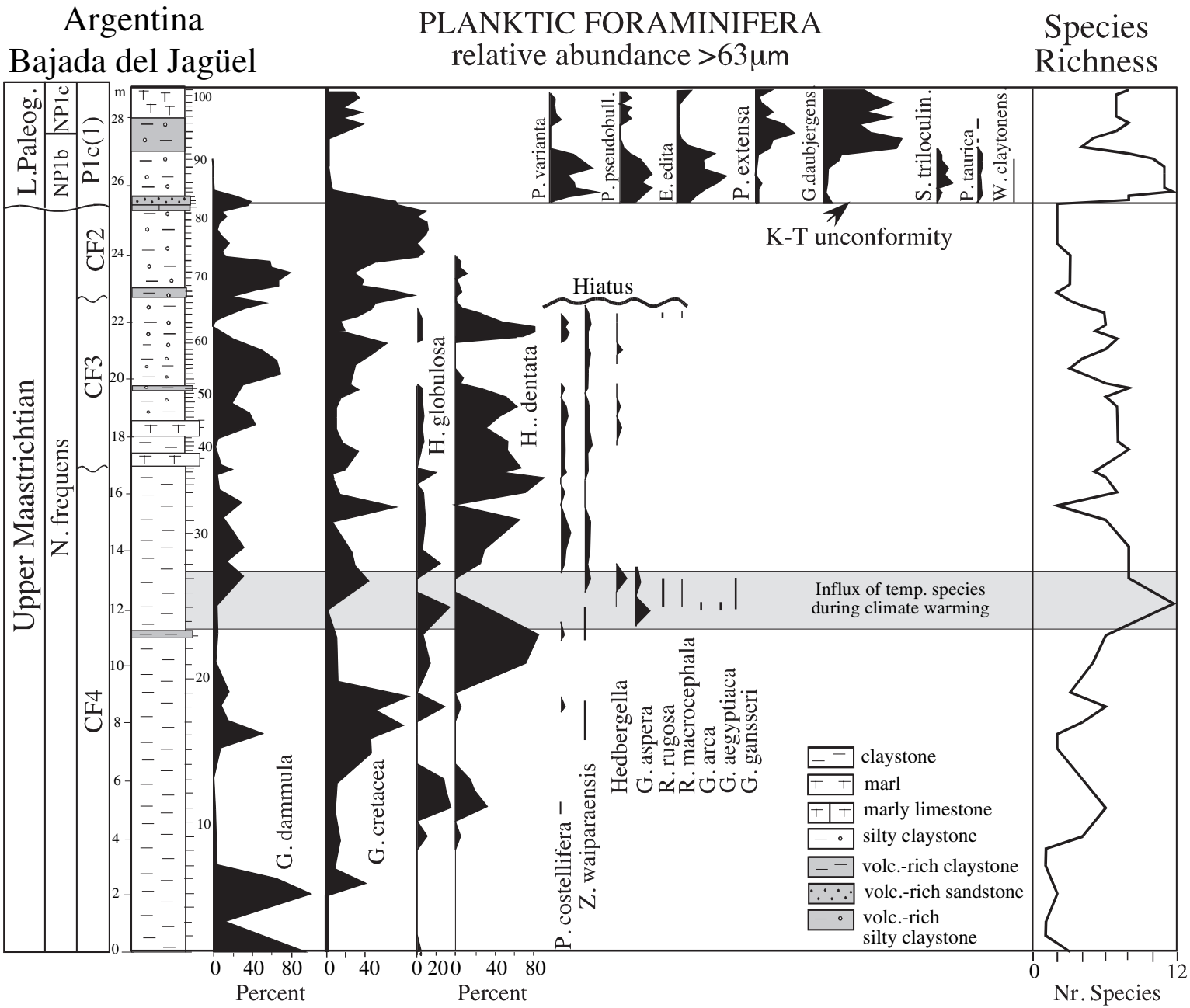

Fig. 6. Relative abundances of planktic foraminiferal species (>63 µm) in the Jagüel section. Note the unusually low species diversity (2-13 species) compared with 35-45 species in comparable southern latitudes during the Maastrichtian. Low species diversity, alternating blooms of the disaster opportunists *Guembelitria* and low oxygen tolerant *Heterohelix* indicate high stress environmental conditions. The temporary incursion of temperate species marks a global warm interval. The K/T boundary interval is missing due to a major unconformity.

Table 2
Relative species abundances of planktic foraminifera (>63 μm) in the upper Maastrichtian and lower Paleocene of the Jagüel section of the Neuquén Basin, Argentina (*number of specimens in samples where foraminifera are rare)

Biozones	CF4																								
Samples: Jagüel (BJ)	1	2	3	4	5	6	7	8	9	10	11	12	13	14	15	16	17	18	19	20	21	22	23	24	25
Guembelitria cretacea				5	1	39			14		7		11		47	46	80	53	85	8	6		8		×
Guembelitria dammula	97		100	5	99	61	100		72		13		43		53	49	18	10	15	4	1		3		2
Heterohelix globulosa	2			1		<1			10		39		27			1	×	28	×	32	15		3		36
Heterohelix dentata	1	none						none	4	none	37	none	16	none				4		54	77	none	83	none	30
Heterohelix planata											2														11
Pseudoguembelina costellifera											2							3		2			3		
Zeauvigerina waiparaensis																2	1	2			×		×		1
Globigerinelloides aspera																									16
Globigerinelloides ultramicra																									2
Hedbergella monmouthensis																									
Globotruncana arca																									×
Globotruncana aegyptiaca																									×
Gansserina gansseri																									×
Rugoglobigerina macrocephala																									×
Total counted	122	0	22	11	155	180	20	0	29	0	102	0	44	0	15	112	111	158	144	134	150	0	275	0	212

Biozones	CF4												CF3												
Samples: Jagüel (BJ)	26	27	28	29	30	31	32	33	34	35	36	37	38	39	40	41	42	43	44	45	46	47	48	49	50
Guembelitria cretacea		41	30	23	21	5	70	14		5	5	20		32	31	18		7		7		7		13	
Guembelitria dammula		36	16	32	10	9	30	4		2	20	7		2		5		42		29		20		26	
Heterohelix globulosa			24	4	41	7		6		×	20	×		3		5		3		3		5		2	
Heterohelix dentate	none	×	24	29	24	62		71	molds	92	49	63	molds	55	68	55	molds	30	too	42	none	61	none	53	none
Heterohelix planate								×											few						
Pseudoguembelina costellifera			4	6	2	10		3		×	6	4		4		4		4		7		5		2	
Zeauvigerina waiparaensis		5	2	5	2	7		×		1		5		2		11		9		9		4		3	
Globigerinelloides aspera		4																							
Hedbergella holmdelensis		4																							
Hedbergella monmouthensis		9		1										×		×		4		2		×			
Globotruncana arca																									
Globotruncana aegyptiaca																									
Rugoglobigerina macrocephala		×												×											
Total counted	0	108	131	149	179	155	108	268	0	225	152	207	0	182	45	140	0	105	0	73	0	200	0	155	0

Biozones	CF3																	CF2								
Samples: Jagüel (BJ)	51	52	53	54	55	56	57	58	59	60	61	62	63	64	65	66		67	68	69	70	71	72	73	74	75
Guembelitria cretacea	33	23	23		29		42		61		16	14	11	27	41	42		81	58	32	34	24	33	44	85	90
Guembelitria dammula	33	70	69		65		50		20		5	1	3	11	32	52		18	42	63	63	74	55	54	12	9
Heterohelix globulosa	4	2									3	2	1	2												
Heterohelix dentate	23	5	4			none		none			63	76	76	44	23	5		1		5	3	2	12	2	3	1
Heterohelix planate									3																	
Pseudoguembelina costellifera	4										6	7	4	7												
Zeauvigerina waiparaensis	2		4		5		7		10		5	×	4	9	3	1										
Globigerinelloides aspera																										
Hedbergella monmouthensis	1	×					1		6		1				1											
Globotruncana arca																										

Globotruncana aegyptiaca																											
Rugoglobigerina macrocephala																											
Total counted	152	113	138	diss	130	0		118	0		101	diss	181	78	150	74	101	81	109	72	133	103	194	81	114	82	68
Biozones	CF2								P1c(1)																		
Samples: Jagüel (BJ)	76	77	78	79	80	81	82	83	84	85	86	87	88	89	90	91	92	93	94	95	96	97	98	99	100	101	102
Guembelitria cretacea	85	93	96	94	86	91	64	62	38	2*	3	2	1	1	×		1			14	32	12	31	14	20	27	23
Guembelitria dammula	15	7	4	6	14	9	36	38	23	2*	1	1	1	1	1	×		1									
Zeauvigerina waiparaensis														1					4		1	1					
Globoconusa daubjergensis									9	1*	1	1	2		2	12	17	71	76	47	33	62	40	58	66	50	42
Parvularugoglobigerina extensa									2		2	2	5	1	1	1	1	11	18	36	28	7	17	12	5	3	14
Eoglobigerina edita									10	1*	22	33	34	38	23	22	33	9	2	1	2	×	1	1	1	7	12
Parasubbotina pseudobulloides									7	6*	11	31	20	30	25	21	11	3			1	9	5	8	2	8	4
Subbotina moskvini									5	8*	12																
Parasubbotina varianta									5	4*	43	23	21	17	37	29	21				1	7	4	4	3	4	2
Subbotina triloculinoides										1*	4	1	12	7	8	2	2							1			
Eobulloides sp.																5	11								1		
Praemurica taurica											1	3	2	2	1	4	3	5		1		1	1				1
Woodringina claytonensis												2		2	1	2		1									
Woodringina hornerstownensis												1	1														
Total counted	73	112	120	119	107	90	111	116	78	23	171	199	150	192	181	174	100	155	187	165	204	158	129	131	195	164	137

in the Danian volcanic-rich bed (27-28 m) and indicates zone NP1c.

5. Mineralogy

5.1. Bulk rock

The dominant bulk rock composition in the Jagüel section consists of phyllosilicates and calcite, which vary between 15-75% and 0-60%, respectively (Fig. 7). Less abundant components include quartz and feldspars (plagioclase and K-feldspar), as well as gypsum from late diagenetic processes. The average calcite/detritus ratio (C/D = calcite/(quartz + phyllosilicates + feldspars) tracks the Ca content due to the relatively constant detrital component. This composition reflects the predominant claystone lithology with minor marl, silt and sandstone. In the upper Maastrichtian (0-25.5 m), phyllosilicates inversely trend calcite contents. Quartz remains relatively constant (8-15%), except for two significant increases at 9.5 m and 15 m. Plagioclase and K-feldspar remain constant around 5% and 3%, respectively, up to 17.5 m. Above 17.5 m both minerals increase (>4%) and reach a maximum of 23% in a siltstone bed at 21.45 m. The XRD pattern of the plagioclase indicates a constant composition close to ordered albite (<An35) with the position of the 221 peak at 29.6-29.7°. This type of plagioclase is characteristic of andesitic volcanism.

The sandstone that overlies the K/T unconformity has very high plagioclase (54%) and gypsum (37%), but no calcite (0%), little quartz (2%) and reduced phyllosilicates (15%, Fig. 7). The plagioclase composition is nearly the same as in the siltstone bed at 21.45 m. Above this sandstone, calcite remains relatively low (<25%) for the first meter and then gradually increases to pre-K/T values of 45% at 28 m. A third plagioclase peak with 9% K-feldspar, but also 22% quartz, is present in the grey-green siltstone 50 cm above the sandstone. Thus, the Jagüel section reveals three intervals with high plagioclase contents reflecting volcanic episodes at 4 m below the K/T unconformity, the K/T unconformity and 50 cm above it.

5.2. Clay minerals

The <2 μm clay fraction is composed of smectite, illite-smectite mixed-layers (IS), kaolinite, mica, chlorite (Fig. 8). In the Jagüel section, smectite is the dominant clay mineral (37-81%, mean: 61%) followed by kaolinite (8-29%, mean: 15%), mica (4-25%, mean: 12%), chlorite (4-20%, mean: 10%) and very low contents of irregular illite-smectite mixed-layers (0-11%, mean: 3%). Mica, chlorite and kaolinite are characterized by similar trends as shown by the positive and significant correlations between mica and chlorite ($R^2 = 0.71$) and mica and kaolinite ($R^2 = 0.69$). However, there is no significant correlation between smectite and other clay minerals. Therefore, variations in clay minerals can be expressed by the ratio of smectite/(kaolinite + chlorite + mica).

Four characteristic intervals are present in the analyzed sequence: (1) the interval from 0-8 m is characterized by low

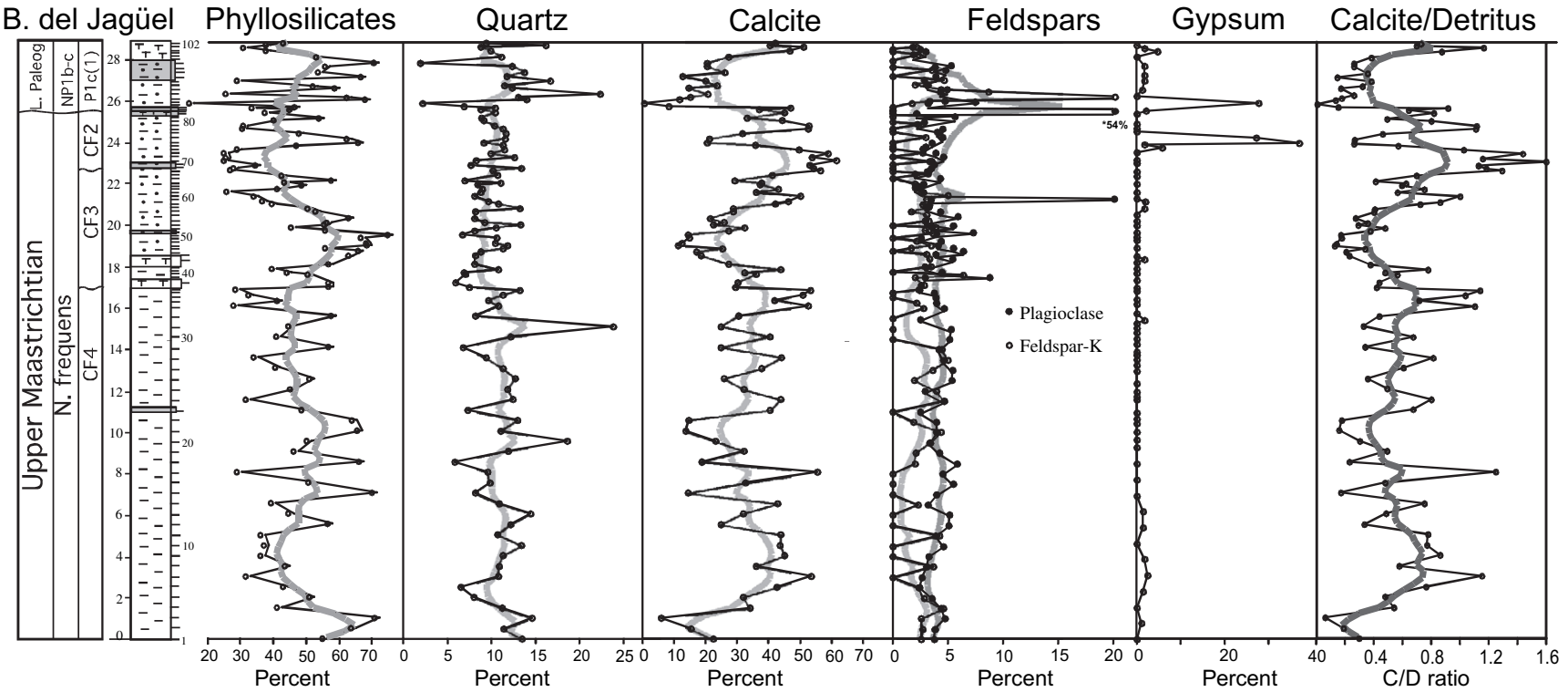

Fig. 7. Bulk rock composition in the Jagüel section. The dominant components are phyllosilicates and calcite. Plagioclase and K feldspars are common and reach peak values in the volcaniclastic sandstone above the unconformity and in intervals 0.5 m above and 4 m below. See legend for lithology on Fig. 6.

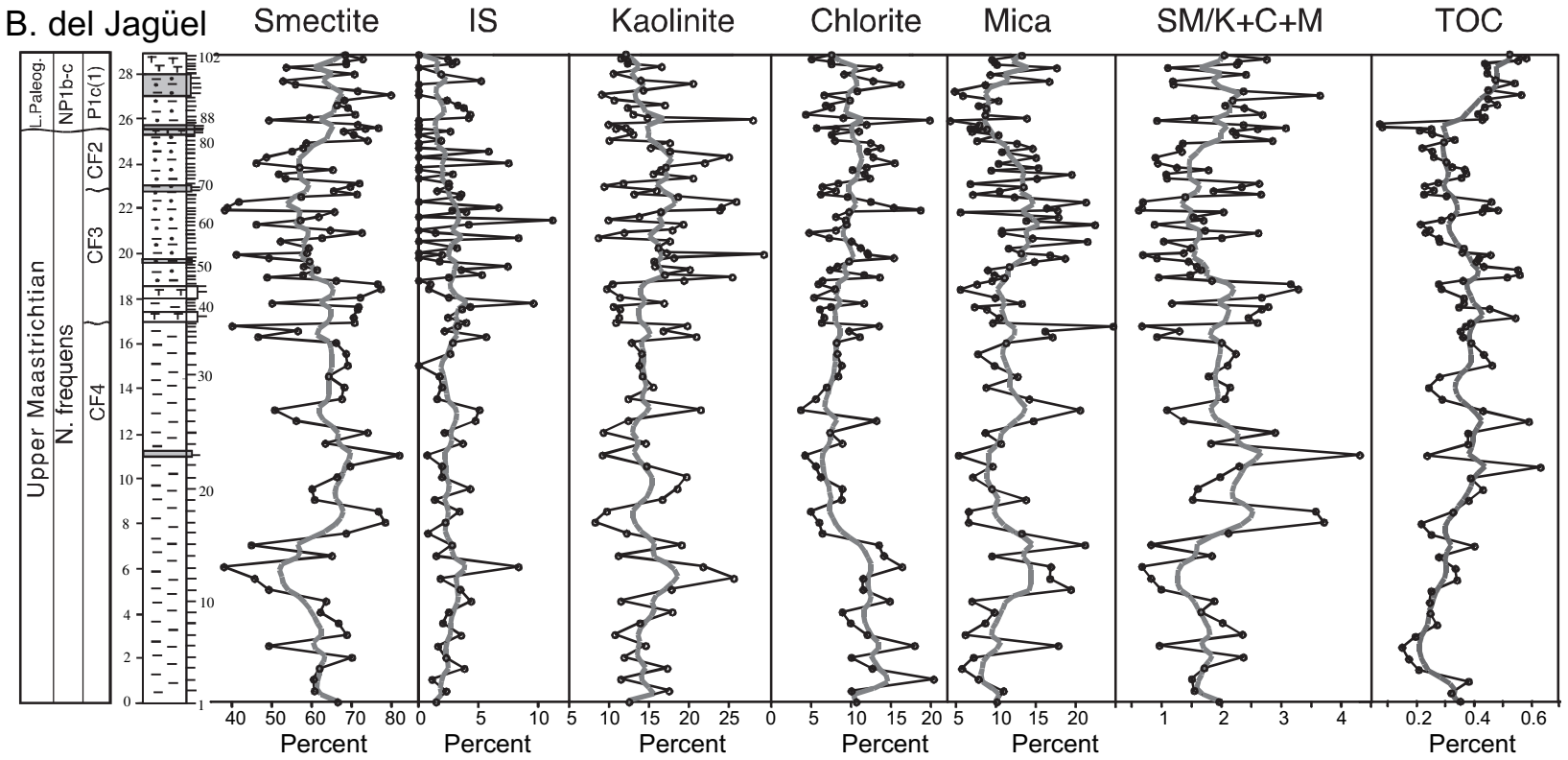

Fig. 8. Clay mineralogy (<2 μm) and TOC values in the Jagüel section. Smectite is the dominant clay mineral and peak values correspond to high TOC. The high smectite content is mainly due to weathering of volcanic matter. See legend for lithology on Fig. 6. Sm/K + C + M = smectite/kaolinite + chlorite + mica.

smectite (37-68%), increased chlorite, mica and kaolinite and consequently low smectite/(kaolinite + chlorite + mica) ratio. (2) Smectite increases up to 80%, to the detriment of chlorite and kaolinite, between 8-18.6 m. (3) Decreasing smectite, but increasing mica, chlorite and at a lesser extent kaolinite, mark the interval between 18.6-25 m. (4) In the Danian part of the section, which includes the volcanic-rich sandstone above the K/T unconformity, smectite increases to the detriment of kaolinite and mica. Apart from these long-term trends, the CF4-CF3, CF3-CF2 and the K/T transitions are marked by significant increases in smectite contents.

5.3. Total organic carbon

Organic carbon and Rock-Eval pyrolysis data indicate that average total organic carbon (TOC) values increased from 0.2 wt% to 0.4 wt% in the lower part of zone CF4 and decrease to 0.3 wt% in the upper Maastrichtian CF3-CF2 interval (Fig. 9). The lowest TOC values (<0.1 wt%) occur within the volcanic-rich sandstone that overlies the K/T unconformity. Maximum average TOC values (0.4 to 0.58 wt%) occur in the Danian (zone P1c) above the sandstone. Rhythmic TOC variations with values as low as 0.15 wt% and as high as 0.7 wt% (Fig. 8) suggest that the TOC was derived from adjacent continental areas.

Information on the composition and maturity of organic carbon can be obtained by pyrolytic measurements (Espitalié et al., 1986; Behar et al., 2001). With this method the type of organic matter is determined by the hydrogen index (HI) and oxygen index (OI), which approximate the H/C atomic ratio and O/C atomic ratio, respectively. Based on the observed range of HI-values (0 to 85 mg HC/g TOC) and of OI-values (135 to 510 mg CO_2/g TOC), the organic matter of the Jagüel section is distributed in the organic matter type III (Fig. 9), which is associated with terrestrial environments (Espitalié et al., 1986). However, high OI values may also indicate significant alteration and oxidation of organic matter during erosion and transport processes, which makes the oxygen index unreliable. If weathering affected the organic matter in the Jagüel section, then a marine source is also likely. Weathering of the organic content is suggested by the low TOC values at times of high marine productivity reflected in $\delta^{13}C$ values (Fig. 10). Given the potential for weathered organic content, the observed TOC increase may only be the remnants of considerable organic matter accumulation due to low oxygen conditions, as suggested by *Heterohelix* blooms (Fig. 6).

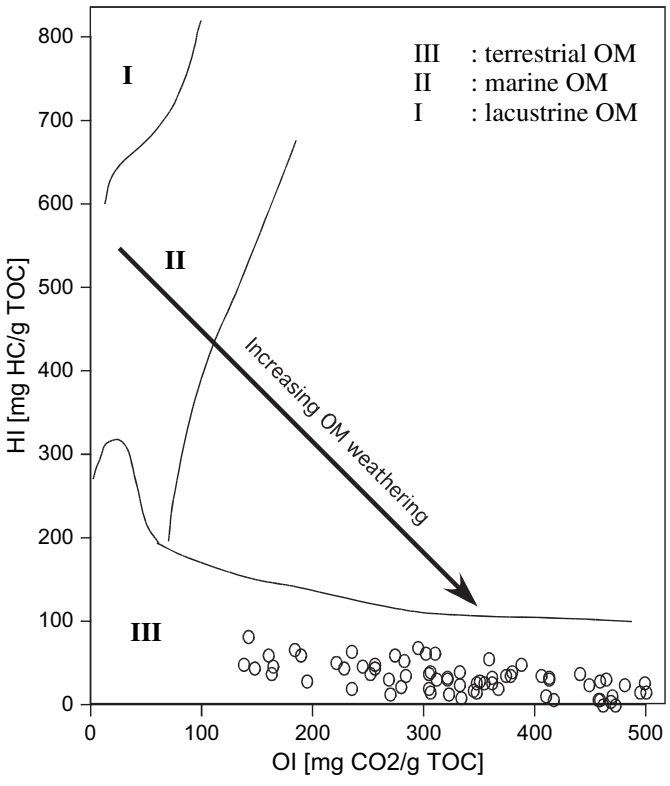

Fig. 9. Hydrogen and oxygen index (HI, OI) in the Jagüel section suggest that the organic matter is of terrestrial origin. However, weathering of organic matter makes this index unreliable and may suggest a marine origin.

6. Stable isotopes

6.1. Carbon isotopes

Carbon and oxygen isotope analysis of the Bajada del Jagüel section was conducted on whole rock fine fraction sediments (<38 μm, Fig. 10). The Jagüel whole rock record can be compared with coeval stable isotope records based on planktic and benthic foraminifera from the shallow water Amboanio Quarry section of the Mahajanga Basin in Madagascar (Abramovich et al., 2002) and South Atlantic DSDP Site 525A (Li and Keller, 1998a). The Jagüel bulk rock $\delta^{13}C$ values are variable averaging between 1.3 and 2‰ for the late Maastrichtian zones CF4 and CF3 and gradually decrease to 0 in zone CF2 (Fig. 10). At Amboanio, $\delta^{13}C$ values are relatively steady around 1.3‰ in zone CF4 and gradually decrease to 0.5‰ near the top of the zone. In zone CF3-CF2, $\delta^{13}C$ values gradually decrease from 1.5‰ to 0.2‰ at the CF2 unconformity.

Carbonate $\delta^{13}C$ excursions are generally interpreted as changes in marine surface productivity. The Jagüel and Amboanio $\delta^{13}C$ values are comparable to benthic values of Site 525A, but are substantially lower than the planktic values, which average between 2-2.5‰ (Li and Keller, 1998a). This suggests that productivity in the two shallow basins of the Neuquén and Mahajanga basins was relatively low compared with the open marine environment of the South Atlantic. The overall low productivity can be explained by the shallow depositional environment and differential fractionation of $\delta^{13}C$ compared with open ocean environments. Abramovich et al. (2002) attributed the decrease in $\delta^{13}C$ values near the top of CF4 in the Amboanio section to gradual shallowing.

6.2. Oxygen isotopes

Bulk rock $\delta^{18}O$ values in zone CF4 of the Jagüel section average between −3 and −4‰ and are comparable to benthic values at the shallow Amboanio section, but lighter than benthic and planktics at the deep water Site 525A (Fig. 10). The CF4/CF3 transition (hiatus) shows heavier values in all three

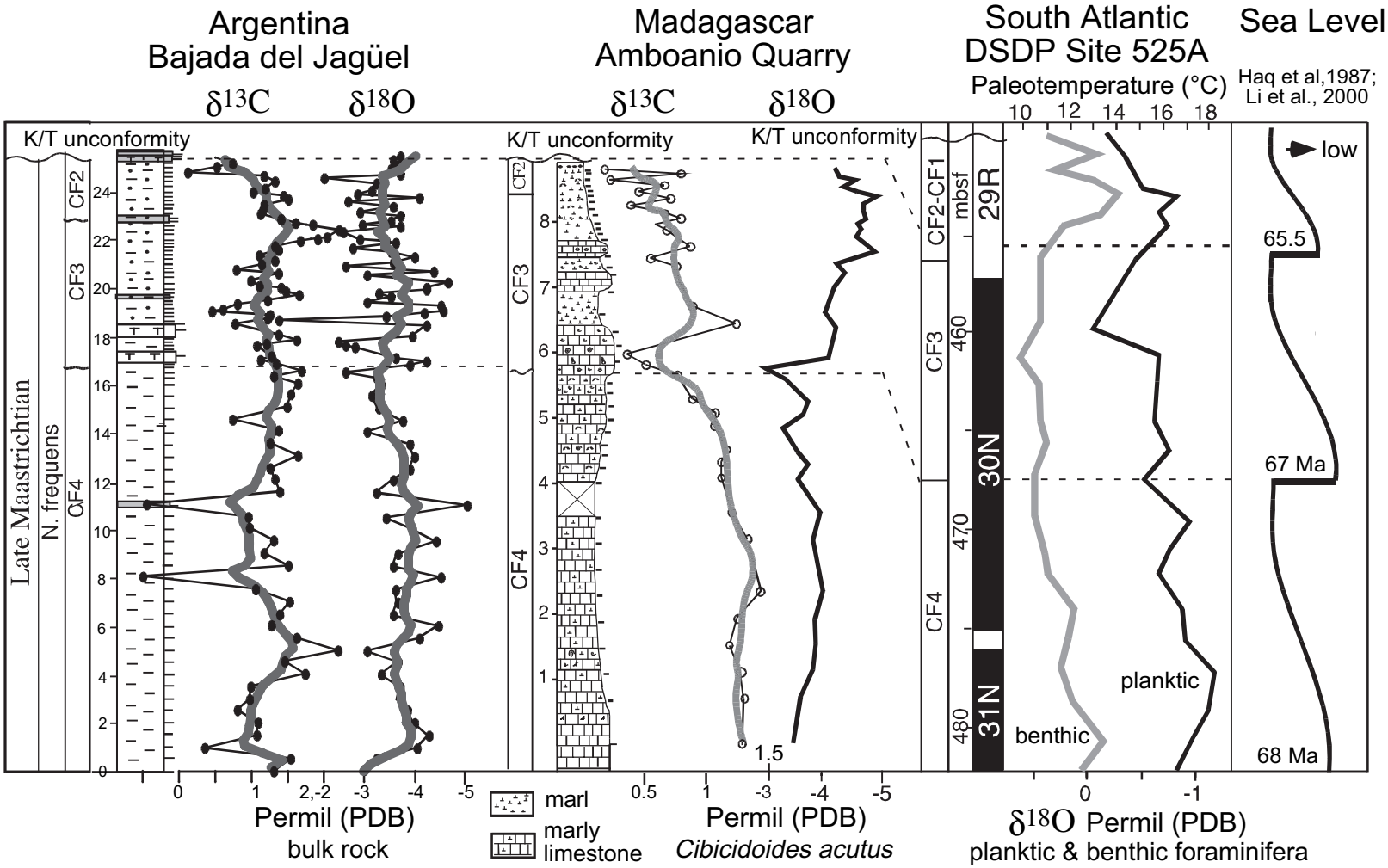

Fig. 10. Correlation of carbon isotope records from the Jagüel section with those from Amboanio, Madagascar (Abramovich et al., 2002) and DSDP Site 525 (Li and Keller, l998a) in the South Atlantic. All three records are from similar palaeolatitudes. See legend for lithology on Fig. 6.

sections. In CF3, $\delta^{18}O$ values decrease to $-4‰$ and $-4.5‰$ in the Jagüel and Amboanio sections, respectively, and increase across the CF3/CF2 transition (hiatus) at Jagüel. Erosion may account for the absence of the upper CF3 increase at Amboanio. At Site 525A $\delta^{18}O$ values decrease in the lower part of CF3, but increase in the upper part in planktic values. The dramatic warming in zone CF1 is not present in the Jagüel or Amboanio sections because this interval is missing at the K/T unconformity in these sections.

The lower $\delta^{18}O$ values could be explained by lower salinity due to fresh water influx in the relatively restricted Neuquén and Mahajanga basins. Alternatively, it could be explained by the presence of some authigenic carbonate, which may form (close to the water sediment interface) in a sulfate-reducing environment, as documented by the common presence of pyrite framboids in the Jagüel section (e.g., Wilkin et al., 1996; Ohfuji and Rickard, 2005). The mineralization of organic matter during bacterial sulfate reduction in organic-rich rocks may produce carbonates with an isotope composition depleted in $\delta^{18}O$ that is compatible with the observed low bulk rock values (Sass et al., 1991).

The Maastrichtian climate record is well known and Site 525A provides an excellent middle latitude record. The main trend is a progressive cooling through the Maastrichtian that culminates near the CF2/CF3 zone boundary (65.5 Ma) and is followed by a short warm event ($\sim$65.2-65.4 Ma) generally attributed to Deccan volcanism (Li and Keller, 1998a,b; Kucera and Malmgren, 1998; Olsson et al., 2001; Abramovich and Keller, 2003). A less dramatic earlier warm event occurs in the early late Maastrichtian zone CF5 to CF4 at Sites 525A, 463 and in terrestrial sequences (Li and Keller, 1999; Nordt et al., 2003). Sea level regressions coincide with major cooling episodes in continental shelf sequences during the late Maastrichtian at $\sim$68 Ma, $\sim$67 Ma and $\sim$65.5 Ma (Haq et al., 1987; Li et al., 2000). The 67 Ma and 65.5 Ma regressions coincide with the CF4/CF3 and CF3/CF2 hiatuses in the Neuquén and Mahajanga basins.

7. Discussion

7.1. Depositional environment inferred from mineralogy

High detrital influx (phyllosilicates and quartz) is generally associated with increased erosion and transport during a sea-level regression and seasonally cool climate, whereas high carbonate deposition is associated with transgressive seas and warm humid climates. In the Jagüel section, this trend is not consistently observed. The two sea level regressions correspond with high calcite/detritus ratios, relatively low pyllosilicate contents and low smectite/(kaolinite + chlorite + mica) ratios (Fig. 11). High sea levels frequently correspond with relatively low calcite/detritus ratios and predominantly higher phyllosilicates (mainly smectite). But high amounts of phyllosilicates do not always correspond to coeval increases of coarser material, such as quartz, which is generally more abundant during regressions. This suggests that the inverse trend may be due to carbonate dilution by the extremely high amounts of phyllosilicates remobilized during the sea level transgression on low relief land areas coupled with weathering of volcanic rocks.

The presence of abundant smectite is generally linked to transgressive seas and warm climate with alternating humid and arid seasons, but can also reflect volcanic activity (Chamley, 1989,1997; Deconinck, 1992). The origin and deposition of smectite depends on several factors. During a sea-level rise, smectite is reworked from soils and enriched by differential settling in open environments (Fig. 12). Chlorite, kaolinite and mica are deposited close to shorelines, while smectites are transported away from shores (Gibbs, 1977; Adatte and Rumley, 1989). Increased smectite therefore reflects high sea levels (Chamley et al., 1990), whereas increased kaolinite, chlorite and mica suggest low sea levels (see smectite/(kaolinite + chlorite + mica ratios, Fig. 11). Abundance of detrital smectite inherited from soils and exported to the open ocean during high sea-levels, indicates the presence of extended low relief land areas to the north and volcanic activity to the southwest (Fig. 1), characterized by a relatively hot climate and seasonal changes in humidity. These processes can easily explain the observed smectite/(kaolinite + chlorite + mica). ratio fluctuations in the Jagüel section.

Submarine alteration of volcanic or impact glass and ash is frequently invoked to explain the widespread occurrence of smectite, often associated with zeolites (clinoptilolite) and opal-CT in marine environments (Weaver and Beck, 1977), especially during the extensive Cretaceous sea level rise linked to high spreading rates and volcanism. A global increase in volcanism coincident with a high sea-level and consequently flooding of land areas is therefore a major contributing factor to the enrichment of smectite in marine conditions (Thiry and Jacquin, 1993). The smectite in the Neuquén Basin may be derived partly from argillized submarine volcanic rocks from the nearby volcanic arc (Figs. 1, 12). Authigenesis of smectite seems unlikely, because it does not explain the variations and disappearance of detrital clays during times of high or low sea levels. Diagenetic alteration of clays is also unlikely because Tertiary deposits in this area do not exceed 1000 m (Bertels, 1970), and hence there was no deep burial diagenesis, which occurs at depths >2 km (Chamley, 1997). Absence of diagenetic overprints due to burial diagenesis is indicated by the constant presence, but variable amounts, of smectite, the co-existence of smectite with high amounts of kaolinite, and the low amounts of mixed layered illite-smectite (Fig. 8).

The detrital and volcanic inputs are therefore the dominant factors for clay mineral distributions in marine sediments of the Jagüel section. Mica and chlorite are considered common byproducts of weathering reactions with low hydrolysis typical of cool to temperate and/or dry climates. Kaolinite is generally a byproduct of highly hydrolytic weathering reactions in perennially warm humid climates. However, relative abundances characterizing kaolinite, chlorite and mica never exceed 25-30% for each mineral, which may result from erosion of older sediments and soils, which increases during regressions. These clay minerals, therefore, do not always reflect palaeoclimatic changes.

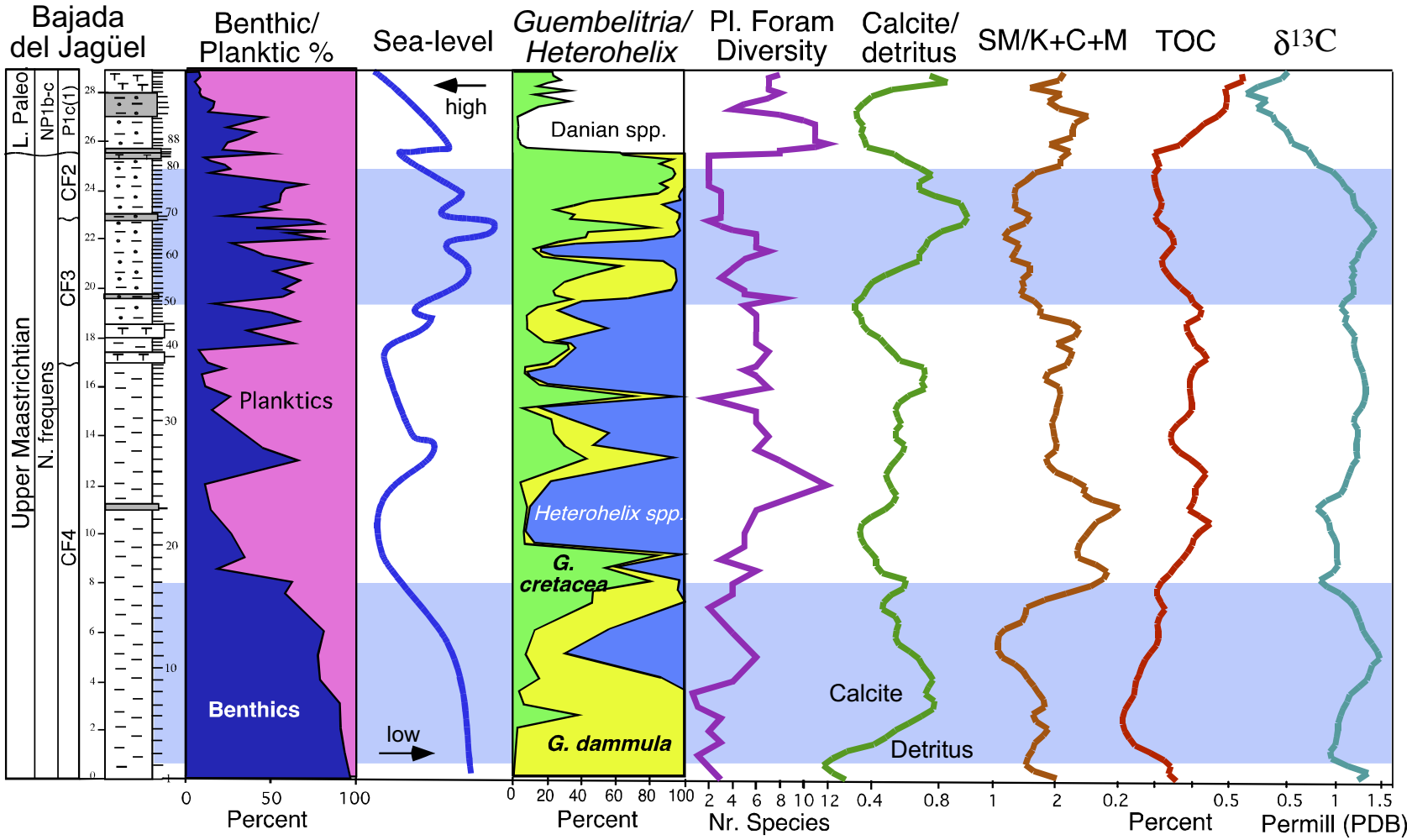

Fig. 11. Environmental proxies based on benthic and planktic foraminifera, sea level changes, mineralogy and geochemistry. High sea levels correspond to low values in the calcite/detritus index, but high TOC, low $\delta^{13}C$ and *Heterohelix* blooms. Low sea levels correspond to high calcite/detritus index, low TOC, high $\delta^{13}C$ and *Guembelitria* blooms. Shaded intervals mark sea level lows. See legend for lithology on Fig. 6.

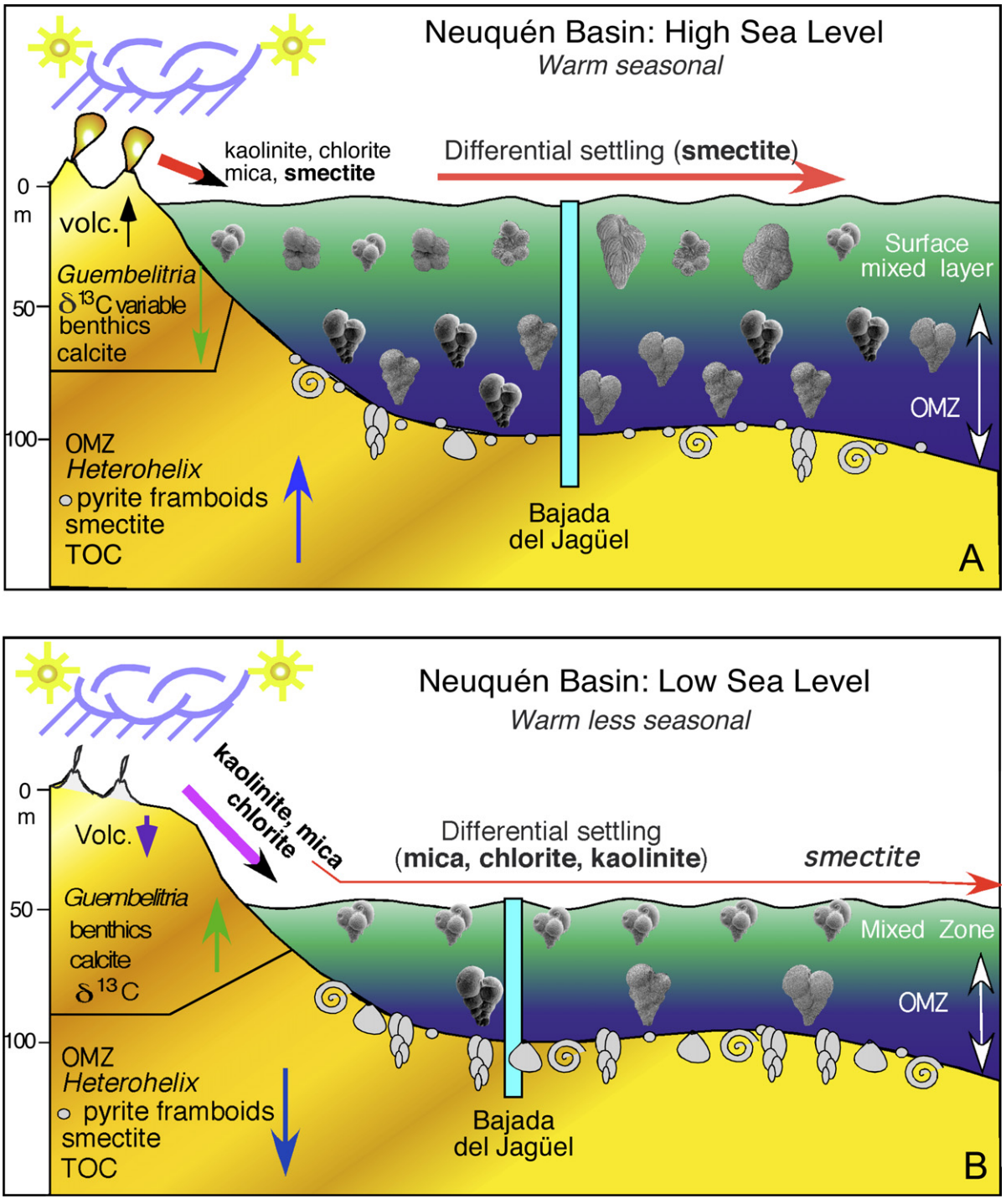

Fig. 12. Schematic depiction of low and high sea level conditions in the Neuquén Basin during the late Maastrichtian. Note that low sea levels are associated with low volcanic activity, high calcite, high benthic abundance and *Guembelitria* blooms in the surface mixed layer. Conversely, high sea levels are associated with high volcanic activity, high smectite input, *Heterohelix* blooms and lower benthic foraminiferal abundance indicating dysaerobic conditions and/or an expanded oxygen minimum zone.

7.2. Palaeoenvironment inferred from microfossils

7.2.1. Benthic foraminifera

Benthic foraminifera are generally most abundant in shallower waters and decrease in deeper waters, whereas planktic foraminifera show the reverse trend. In the Jagüel section, benthic foraminifera indicate two intervals of relatively shallow waters in the lower CF4 and CF3/CF2 zones (Fig. 11). The CF3/CF2 transition is marked by a hiatus and coincides with the well-documented global cooling and sea level regression at 65.5 Ma (Haq et al., 1987; Barrera and Huber, 1990; Li et al., 2000). Both shallow water periods are marked by *Guembelitria*

blooms in the surface mixed layer, high abundances of dwarfed low oxygen tolerant benthic foraminifera (e.g. buliminellids, bolivinids and agglutinated species), variable presence of macrofossils (echinoids, gastropods, ostracods and bivalves, such as *Nucula*, *Panopea*, and *Malletia*), the trace fossil *Chondrites* and framboidal pyrite. These assemblages indicate dysoxic conditions, as also indicated by the framboidal pyrite (Wignall et al., 2005; Wilkin et al., 1996). Deposition occurred in a middle neritic environment (Bertels, 1975), probably no deeper than ~100 m. A higher sea level is indicated by the low benthic abundance in the upper zone CF4, as also suggested by an influx of temperate species, including globotruncanids, rugotruncanids and archaeoglobigerinids (Fig. 6) and peak planktic diversity. This interval corresponds to a period of global warming (Barrera and Huber, 1990; Li and Keller, 1998a; Nordt et al., 2003). Above the K/T unconformity, zone Plc indicates a higher sea level (low benthic abundance) and dysaerobic seafloor, as indicated by dwarfed, low oxygen tolerant benthic species (mostly buliminellids and *Epistominella minuta*).

7.2.2. Guembelitria *and* Heterohelix *blooms*

Planktic foraminifera of the Neuquén Basin of Argentina reveal unusually high-stress late Maastrichtian assemblages dominated by *Guembelitria*, a disaster opportunistic group that thrived in environments where few or no other species survived. *Guembelitria* blooms, are generally considered indicative of the post-K/T mass extinction, where *Guembelitria cretacea* is the only Cretaceous species that thrived in the aftermath of the mass extinction and prior to the evolution and diversification of the new Tertiary fauna. More recently, *Guembelitria* blooms have also been documented from various late Maastrichtian sequences in shallow and deep waters, marginal seas and upwelling areas as well as in volcanically active regions (e.g., Bulgaria, Egypt, Madagascar, Ninetyeast Ridge Site 216, Abramovich et al., 2002; Adatte et al., 2002; Keller, 2002, 2003; Keller and Pardo, 2004). But they are most widespread in shallow nearshore areas. *Guembelitria* thrived in environments that are generally toxic to other species, possibly because of eutrophic conditions, which may result from high terrigenous runoff, stagnant oceanic basins, upwelling of nutrient-rich waters, phosphorus input from volcanism, or any combination thereof. The frequent presence of *Guembelitria* blooms during the late Maastrichtian in the Neuquén Basin (Figs. 6, 11) thus reveals intermittent high-stress conditions. When other species are present, they are generally dwarfed, which is considered a result of high-stress (MacLeod et al., 2000; Twitchett et al., 2001).

Previous studies have shown that *Guembelitria* blooms are generally followed by blooms of biserial low oxygen tolerant species (*Heterohelix globulosa* and/or *H. dentata*), which subsequently yield to small trochospiral and planispiral forms (*Globigerinelloides*, *Hedbergella*), followed by the return of more diverse, larger species as the environment gradually returns to normal (oligotrophic) conditions (Keller and Pardo, 2004). *Heterohelix* species generally thrived in subsurface low oxygen environments and their blooms thus indicate oxygen depletion, expansion of the oxygen minimum zone, and/or increased watermass stratification. In the Neuquén Basin *Guembelitria* (*G. cretacea* and *G. dammula*) blooms alternate with *Heterohelix* (*H. globulosa*, *H. dentata*) blooms during the late Maastrichtian and rarely approached environmental conditions more favourable to other (oligotrophic) species. Among these blooms there is a regular and repeated succession from *G. dammula* → *G. cretacea* → *H. dentata* (*H. globulosa* is not abundant enough to show a clear trend, Fig. 6).

The environmental conditions that favored these blooms in the Neuquén Basin are illustrated in Fig. 12. During high sea levels and warm seasonal climates (Figs. 11, 12A), flooding of land areas resulted in the enrichment of smectite in the marine environment derived partly from argillized submarine volcanic rocks from the nearby volcanic arc. The surface mixed zone supported a variety of species, but relatively low *Guembelitria* abundance, and $\delta^{13}C$ values were relatively low but variable. *Heterohelix* thrived in an expanded oxygen minimum zone (OMZ) to the exclusion of other species. On the sea floor, reduced assemblages of low oxygen tolerant benthic foraminifera survived in organic-rich (high TOC) sediments with common pyrite framboids, which indicate a dysoxic benthic environment (Fig. 12A). During times of lower sea level, warm and less seasonal climates prevailed, with reduced smectite, but increased kaolinite, chlorite and mica in the marine environment (Fig. 12B). $\delta^{13}C$ values are higher and *Guembelitria*, which favour nearshore nutrient-rich environments, thrived in the surface mixed zone. Reduced abundances of *Heterohelix*, decreased TOC and pyrite framboids suggest a reduced OMZ, though still dysoxic benthic environment (Fig. 12B).

7.2.3. Micula decussata, Thoracosphaera *and* Braarudosphaera *blooms*

Micula decussata is the most dominant nannofossil species in the late Maastrichtian of the Neuquén Basin in Argentina and similar blooms have been observed in sections from low to high latitudes and shallow to deep-water environments (Eshet et al., 1992; Gardin and Monechi, 1998; Gardin, 2002; Tantawy, 2003a,b). It has been suggested that *M. decussata* blooms are partly artefacts of dissolution of less robust forms (e.g., *A. cymbiformis* and *K. magnificus*) Eshet and Almogi-Labin (1996). However, in the well-preserved assemblages of the Jagüel section, DSDP Site 216, Israel and Egypt delicate and solution-susceptible taxa are present (e.g., *Nephrolithus frequens*, *C. ehrenbergii*, *P cretacea*, *A. octaradiata E. turiseiffelii*) and the dissolution resistant *Watznaueria barnesae* is rare, suggesting that dissolution effects are not the sole factor controlling *M. decussata* abundance. Alternatively, *Micula decussata* may be a high stress survivor of yet unknown environmental affinity.

Thoracosphaera and *Braarudosphaera bigelowii* dominate the early Danian in the Jagüel section with alternating peaks varying between 41% and 94% (Fig. 5). Blooms of *Thoracosphaera* are known from middle to low latitudes (Perch-Nielsen et al., 1982; Jiang and Gartner, 1986; Gardin and Monechi, 1998; Tantawy, 2003a,b). In the Jagüel section, this species shows a sudden increase in relative abundance to 48%, and a parallel rapid decrease in Cretaceous species richness in the 1.2 m above the K/T boundary. *Thoracosphaera* is considered an opportunistic species that tolerates unusual marine

conditions, including major changes in primary productivity and salinity (Eshet et al., 1992; Gaarder and Hasle, 1971). *Braarudosphaera bigelowii* shows two peak abundances of about 72% in the Danian of the Jagüel section (Table 1, Fig. 5). These blooms follow the *Thoracosphaera* bloom in low to middle latitude. *Braarudosphaera bigelowi* blooms may indicate nearshore depositional environments characterized by relatively shallow water, increased fresh-water influx or eutrophication (Thierstein and Berger, 1979; Müller, 1985).

7.3. K/T boundary event

There is general agreement among reports on the Neuquén Basin sections that the K/T boundary in the Jagüel section coincides with the unconformity at the base of a 15-25 cm thick volcaniclastic sandstone bed. What is uncertain is the extent of the missing interval at this unconformity and the nature and origin of the sandstone. Palamarczuk and Habib (2001) first interpreted this layer as a plagioclase sand of possible tsunami origin, but subsequently reconsidered this interpretation describing it as of volcanic origin and dominated by pyroclastics (Palamarczuk et al., 2002). A volcanic origin of this sandstone is confirmed by our study by the high amounts of plagioclase of mainly albite composition and glass shards. Recently, Scasso et al. (2005) interpreted this volcaniclastic sandstone as a tsunami deposit generated by the Chicxulub impact on Yucatan. In the absence of impact signals (e.g., iridium, spinels, PGEs, impact glass), their interpretation is based on the presence of rip-up clasts, normal grading and hummocky cross-bedding in the sandstone and a macrofossil ''dead zone'' above it. We agree that these sedimentary features indicate storm deposition, as is common in shallow water sequences during regressions (Yancey, 1996; Gale, 2006), but find no evidence for an impact origin. Both nannofossil and planktic foraminiferal biostratigraphies indicate that the early Danian is missing and therefore no ''dead zone'' related to the K/T impact can be inferred.

8. Summary

During the late Maastrichtian to early Paleocene, the Jagüel section was located in the Neuquén embayment with an active volcanic arc to the West that experienced continuous volcanic activity with several major eruptions, as evident by the presence of five volcanic-rich beds in the studied interval. An extensive land area to the NE created favourable conditions for a warm climate with seasonal changes in humidity, as suggested by clay mineralogy, and an open seaway to the South Atlantic maintained marine conditions. In this environment, the presence of a volcaniclastic sandstone above the K/T unconformity was not unique. At least three such beds with similar mineralogical compositions and high volcanic input were deposited during the late Maastrichtian to Danian and partly reworked during sea-level fluctuations and storms. The K/T boundary interval appears to be missing due to an unconformity that spans from the early Danian (zones P1c, NP1b) through the latest Maastrichtian zones CF1 and *Micula prinsii*. The erosive base of this unconformity, the rip-up clasts, normal grading and hummocky cross bedded sandstone are common features associated with sea level regressions and/or storm deposits in shallow water environments. Sediment deposition occurred in relatively shallow middle neritic ($\sim$100 m) depths in dysoxic bottom waters, as indicated by low oxygen tolerant benthic foraminifera and common pyrite framboids. Alternating blooms of the disaster opportunists *Guembelitria* and low oxygen tolerant *Heterohelix* groups indicate nutrient-rich surface waters and an oxygen depleted water column during low and high sea levels, respectively. High stress conditions were probably driven by high nutrient influx from marine, terrestrial and volcanic origins.

Acknowledgements

We thank four anonymous reviewers for their critiques and suggestions for improvement. We are gratefule to Arturo Quinzio-Sinn and Christian Salazar-Soto for many lively discussions, field assistance in Argentina, logistical support, and for making facilities available at the Geology Department of the University of Concepción, Chile. This research was supported by the US National Science Foundation under grant EAR-0207407 (GK), the German Science Foundation grants STI 128/6 and 7 (WS), and STU 169/10-1 to 3 (DS), and the Swiss National Fund No. 8220-028367 (TA).

References

Abramovich, S., Keller, G., 2003. Planktonic foraminiferal response to the latest Maastrichtian abrupt warm event: a case study from South Atlantic DSDP Site 525A. Marine Micropaleontology 48, 225–249.

Abramovich, S., Keller, G., Adatte, T., Stinnesbeck, W., Hottinger, L., Stüben, D., Berner, Z., Ramanivosoa, B., Randriamanantenasoa, A., 2002. Age and paleoenvironment of the Maastrichtian-Paleocene of the Mahajanga Basin, Madagascar: a multidisciplinary approach. Marine Micropaleontology 47, 17–70.

Adatte, T., Stinnesbeck, W., Keller, G., 1996. Lithostratigraphic and mineralogical correlations of near-K/T boundary clastic sediments in northeastern Mexico: implications for mega-tsunami or sea level changes? Geological Society of America Special Paper 307, 197–210.

Adatte, T., Keller, G., Burns, S., Stoykova, K.H., Ivanov, M.I., Vangelov, D., Kramer, U., Stueben, D., 2002. Paleoenvironment across the Cretaceous-Tertiary transition in eastern Bulgaria. Geological Society of America Special Paper 356, 231–252.

Adatte, T., Rumley, G., 1989. Sedimentology and mineralogy of Valanginian and Hauterivian in the stratotypic region (Jura mountains, Switzerland). In: Wiedmann, J. (Ed.), Cretaceous of the Western Tethys. Proceedings 3rd International Cretaceous Symposium. Scheizerbart'sche Verlagsbuchhandlung, Stuttgart, pp. 329–351.

Albertão, G.A., Koutsoukos, E.A.M., Regali, M.P.S., Attrep Jr., M., Martins Jr., P.P., 1994. The Cretaceous-Tertiary boundary in southern low-latitude regions: preliminary study in Pernambuco, north-eastern Brazil. Terra Nova 6, 366–375.

Albertão, G.A., Martins Jr., P.P., 1996. A possible tsunami deposit at the Cretaceous-Tertiary boundary in Pernambuco, Northeastern Brazil. Sedimentary Geology 104, 189–201.

Barrera, E., Huber, B., 1990. . Evolution of Antarctic waters during the Maastrichtian: Foraminifera oxygen and carbon isotope ratios, Leg 113. Proceedings of the Ocean Drilling Program, Scientific Results 113, 813–827.

Behar, F., Beaumont, V., De Pentadeo, B., 2001. Rock-Eval technology: performances and developments. Oil and Gas Science and Technology. Revue de l'Institut Français du Pétrole (IFP) 56 (2), 111–134.

Berggren, W.A., Kent, D.V., Swisher III, C.C., Aubry, M.-P., 1995. A revised Cenozoic geochronology and chronostratigraphy. In: Berggren, W., Kent, D.V., Aubry, M.-P., Hardenbol, J. (Eds.), Geochronology, Time Scales and Global Stratigraphic Correlation. Society for Sedimentary Geology, Special Publication 54, pp. 129−212.

Bertels, A., 1964. Micropaleontología del Paleoceno de General Roca (Prov. de Rio Negro). Revista del Museo de la Plata, Nueva Serie 4, Paleontología 23, 125−184.

Bertels, A., 1970. Los foraminiferos planctónicos de la cuenca Cretácica-Terciaria en Patagonia Septentrional (Argentina), con consideraciones sobre la estratigrafia del Fortín General Roca (Provincia de Río Negro). Ameghiniana 7, 1−47.

Bertels, A., 1975. Bioestratigrafía del Paleogeno en la República Argentina. Revista Espanola de Micropaleontologia 8, 429−450.

Bertels, A., 1979. Paleobiogeografia de los foraminiferos del Cretácico superior y Cenozoico de América del Sur. Ameghiniana 16 (3−4), 273−356.

Bertels, A., 1980. Estratigrafía y foraminíferos (Protozoa) bentónicos del límite Cretácico-Terciario en el área típo de la Formación Jagüel, provincia de Neuquén, República Argentina. Segundo Congreso Argentino de Paleontología y Bioestratigrafía y Primer Congreso Latinoamericano de Paleontología 2, 47−92.

Bertels, A., 1987. Los Foraminíferos del Cretácico de la Republica Argentina. Sus tendencias paleobiogeographicas. Academia National des Ciencias Exactas, Fisicas y Naturales, Anales 37, 265−305.

Bralower, T.J., Siesser, W.G., 1992. Cretaceous calcareous nannofossil biostratigraphy of Sites 761,762, and 763, Exmouth and Wombat plateaus, Northwest Australia. Proceedings of the Ocean Drilling Program, Scientific Results 122, 529−556.

Caron, M., 1985. Cretaceous planktic foraminifera. In: Bolli, H.M., Saunders, J.B., Perch-Nielsen, K. (Eds.), Plankton Stratigraphy. Cambridge University Press, pp. 17−86.

Casadío, S., 1994. Estratigrafia secuencial del limite Cretacico-Terciario en el occidente de la Provincia de La Pampa. Tercera Reunion Argentina de Sedimentologia, Actas 3, 87−93.

Casadío, S., 1998. Las ostras del límite Cretácico-Paleógeno de la cuenca Neuquina (Argentina). Su importancia bioestratigráfica y paleobiogeográfica. Ameghiniana 35 (4), 449−471.

Chamley, H., 1989. Clay-sedimentology. Springer Verlag, Berlin, 623 p.

Chamley, H., 1997. Clay Mineral sedimentation in the Ocean. In: Paquiet, H., Clauer, N. (Eds.), Soils and Sediments. Springer Verlag, pp. 269−302.

Chamley, H., Deconinck, J.F., Millot, G., 1990. Sur l'abondance des minéraux smectitiques dans les sédiments marins communs déposés lors des périodes de haut niveau marin du Jurassique au Paléogène. Comptes Rendus Academie des Sciences Paris 311 (2), 1529−1536.

Deconinck J.F., 1992. Sédimentologie des argiles dans le Jurassique-Crétacé d'Europe occidentale et du Maroc. Mémoire Habilitacion Lille I, 266 p.

Donovan, A.D., Baum, R.G., Blechschmidt, G.L., Loutit, T.S., Pflum, C.E., Vail, P.R., 1988. Sequence stratigraphic setting of Cretaceous-Tertiary boundary in central Alabama. In: Wilgus, C.K., Hastings, B.S., Kendall, C.G., Posamentier, H.W., Ross, C.A., von Wagoner, J.C. (Eds.), Sea Level Changes-an Integrated Approach. SEPM Special Publication 42, pp. 299−307.

Eshet, Y., Almogi-Labin, A., 1996. Calcareous nannofossils as paleoproductivity indicators in Upper Cretaceous organic-rich sequences in Israel. Marine Micropaleontology 29, 37−61.

Eshet, Y., Moshkovitz, S., Habib, D., Benjamini, C., Magaritz, M., 1992. Calcareous nannofossil and dinoflagellate stratigraphy across the Cretaceous/Tertiary boundary at Hor Hahar, Israel. Marine Micropaleontology 18 (3), 199−228.

Espitalié, J., Deroo, G., Marquis, F., 1986. La pyrolyse Rock-Eval et ses applications. Partie 3. Revue Institut Francé du Pétrole 41, 1.

Gaarder, K.R., Hasle, G.R., 1971. Coccolithophorids of the Gulf of Mexico. Bulletin of Marine Science of the Gulf and Caribbean 21 (2), 519−544.

Gale, A., 2006. The Cretaceous-Tertiary boundary on the Brazos River, Falls County, Texas; evidence for impact-induced tsunami sedimentation? Proceedings of the Geologists' Association 117, 1−13.

Gardin, S., 2002. Late Maastrichtian to early Danian calcareous nannofossils at Elles Northwest Tunisia). A tale of one million years across the K/T boundary. Palaeogeography, Palaeoclimatology, Palaeoecology 178, 211−231.

Gardin, S., Monechi, S., 1998. Palaeoecological change in middle to low latitude calcareous nannoplankton at the Cretaceous-Tertiary boundary. Bulletin de la Société Géologique de France 169, 709−723.

Gibbs, R.J., 1977. Clay mineral segregation in the marine environment. Journal of Sedimentary Petrology 47, 237−243.

Haq, B.U., Hardenbol, J., Vail, P.R., 1987. Chronology of fluctuating sea levels since the Triassic. Science 235, 1156−1167.

Hart, M.B., Feist, S.E., Hakansson, E., Heinberg, C., Price, G.D., Leng, M.J., Watkinson, P., 2005. The Cretaceoous-Paleogene boundary succession at Stevns Klint, Denmark: Foraminifers and stable isotope stratigraphy. Palaeogeography, Palaeoclimatology, Palaeoecology 224, 6−26.

Jiang, M.J., Gartner, S., 1986. Calcareous nannofossil succession across the Cretaceous/Tertiary boundary in east-central Texas. Micropaleontology 32 (3), 232−255.

Keller, G., 2001. The end-Cretaceous mass extinction in the marine realm: year 2000 assessment. Planetary and Space Science 49, 817−830.

Keller, G., 2002. *Guembelitria* dominated late Maastrichtian planktic foraminiferal assemblages mimic early Danian in Central Egypt. Marine Micropaleontology 47, 71−99.

Keller, G., 2003. Biotic effects of volcanism and impacts. Earth and Planetary Science Letters 215, 249−264.

Keller, G., 2004. Low diversity late Maastrichtian and early Danian planktic foraminiferal assemblages of the eastern Tethys. Journal of Foraminiferal Research 34 (1), 49−73.

Keller, G., Adatte, T., Berner, Z., Harting, M., Baum, G., Prauss, M., Tantawy, A.A., Stueben, D., 2007. Chicxulub impact predates K-T boundary: new evidence from Texas. Earth and Planetary Science Letters 255, 339−356.

Keller, G., Barrera, E., Schmitz, B., Mattson, E., 1993. Gradual mass extinction, species survivorship and long-term environmental changes across the Cretaceous-Tertiary boundary in high latitudes. Geological Society of America Bulletin 105, 979−997.

Keller, G., Pardo, A., 2004. Disaster opportunists Guembellitrinidae: index for environmental catastrophes. Marine Micropaleontology 53, 83−116.

Keller, G., Li, L., MacLeod, N., 1995. The Cretaceous-Tertiary boundary stratotype section at El Kef, Tunisia: how catastrophic was the mass extinction? Palaeogeography, Palaeoclimatology, Palaeoecology 119, 221−254.

Keller, G., Stinnesbeck, W., Adatte, T., Stueben, D., 2003. Multiple impacts across the Cretaceous-Tertiary boundary. Earth-Science Reviews 62, 327−363.

Keller, G., Adatte, T., Stinnesbeck, W., Rebolledo-Vieyra, M., Urrutia Fuccugauchi, J., Kramar, G., Stueben, D., 2004a. Chicxulub predates the K/T boundary mass extinction. Proceedings of the National Academy of Sciences 101, 3753−3758.

Keller, G., Adatte, T., Stinnesbeck, W., Stueben, D., Berner, Z., Kramar, U., Harting, M., 2004b. More evidence that the Chicxulub impact predates the K/T mass extinction. Meteoritics & Planetary Science 39 (7), 1127−1144.

Kübler, B., 1987. Cristallinité de l'illite, méthods normalisées de préparations, méthodes normalisées de measures. Neuchâtel, Suisse, Cahiers Institute Géologie, Série ADX 1, 13 p.

Kucera, M., Malmgren, B.A., 1998. Terminal Cretaceous warming event in the mid-latitude South Atantic Ocean: Evidence from poleward migration of *Contusotruncana contusa* (planktonic foraminifera) morphotypes. Palaeogeography, Palaeoclimatology, Palaeoecology 138, 1−15.

Legarreta, L., Gulisano, C.A., 1989. Analisis estratigrafico secuencial de la Cuenca Neuquina (Triasico superior-Terciario inferior). In: Chabli, G., Spaletti, L. (Eds.), Cuencas Sedimentarias Argentinas, pp. 221−243.

Li, L., Keller, G., 1998a. Maastrichtian climate, productivity and faunal turnovers in planktic foraminifera in South Atlantic DSDP Sites 525 and 21. Marine Micropaleontology 33, 55−86.

Li, L., Keller, G., 1998b. Abrupt deep-sea warming at the end of the Cretaceous. Geology 26, 995−999.

Li, L., Keller, G., 1999. Variability in Late Cretaceous climate and deep waters: evidence from stable isotopes. Marine Geology 161, 171−190.

Li, L., Keller, G., Adatte, T., Stinnesbeck, W., 2000. Late Cretaceous sea level changes in Tunisia: a multi-disciplinary approach. Journal of the Geological Society (London) 157, 447−458.

MacLeod, N., 1998. Impacts and marine invertebrate extinctions. In: Grady, M.M., Hutchison, R., McCall, G.J.H., Rothery, D.A. (Eds.),

Meteorites: Flux withTime and Impact Effects. Geological Society of London Special Publication, 140, pp. 217−246.

MacLeod, N., Ortiz, N., Fefferman, N., Clyde, W., Schulter, C., MacLean, J., 2000. Phenotypic response of foraminifera to episodes of global environmental change. In: Culver, S.J., Rawson, P. (Eds.), Biotic Response to Global Environmental Change: The Last 145 Million Years. Cambridge University Press, Cambridge, pp. 51−78.

MacLeod, K.G., Whitney, D.L., Huber, B.T., Koeberl, C., 2007. Impact and extinction in remarkably complete Cretaceous-Tertiary boundary sections from Demerara Rise, tropical western North Atlantic. Geological Society of America Bulletin 119 (1), 101−115.

Marini, F., Albertão, G.A., Oliveira, A.D., Delicio, M.P., 1998. Preliminary SEM and EPMA investigations on K/T Boundary spherules from the Pernambuco area (Northeastern Brazil): diagenetic apatite and fluorite concretions, suspected fluorine anomalies. Proceedings of the Annual Meeting Tecos. Akadémiai Kiadó, Budapest, pp. 109−117.

Martins Jr., P.P., Albertão, G.A., Haddad, R., 1998. The Cretaceous-Tertiary boundary in the context of impact and sedimentary record − a review of 10 years of researches in Brasil. Revista Brasileira de Geociências 30 (3), 460−465.

Müller, C., 1985. Biostratigraphic and paleoenvironmental interpretation of the Goban Spur region based on a study of calcareous nannoplankton. Initial Reports of the Deep Sea Drilling Project 80, U.S. Government Printing Office, Washington, 80, 573−599.

Nañez, C., Concheyro, A., 1997. Límite Cretácico-Paleogeno. In: Geología y Recursos Minerales del Departamento Añelo, Provincia de Neuquén, República Argentina. Dirección Nacional del Servicio Geológico, Anales 25 y Dirección Provincial de Minería Boletín 3, 129−149.

Nordt, L., Atchley, S., Dworkin, S., 2003. Terrestrial evidence for two greenhouse events in the latest Cretaceous. GSA Today 13, 4−9.

Norris, R.D., Huber, B.T., Self-Trail, J., 1999. Synchroneity of the K/T oceanic mass extinction and meteorite impact: Blake Nose, western North Atlantic. Geology 27, 419−422.

Ohfuji, H., Rickard, D., 2005. Experimental synthesis of framboids − a review. Earth-Science Reviews 71, 147−170.

Olsson, R.K., Hemleben, C., Berggren, W.A., Huber, B.T., 1999. Atlas of Paleocene planktonic foraminifera. Smithsonian Contribution to Paleobiology No. 85. Smithonian Insstitution Press, Washington, DC, 252 p.

Olsson, R.K., Wright, J.D., Miller, K.G., 2001. Paleobiogeography of *Pseudotextularia elegans* during the latest Maastrichtian warming event. Journal of Foraminiferal Research 31, 275−282.

Palamarczuk, S., Habib, D., 2001. Dinoflagellate evidence of the Cretaceous-Paleogene boundary in Argentina. Geological Society of America, Annual Meeting, Nov. 5-8, 2001. Web page.

Palamarczuk, S., Habib, D., Olsson, R.K., Hemming, S., 2002. The Cretaceous-Paleogene boundary in Argentina: New evidence from dinoflagellate, foraminiferal and radiometric dating. Geological Society of America Abstracts with Program. No. 61−20.

Papú, O.H., Prámparo, M.B., Nañez, C., Concheyro, A., 1999. Palinología y micropaleontología de la Formacíon Jagüel (Maastrichtiano-Daniano), perfil Opazo, cuenca Neuquina, Argentina. Simposio Paleógeno de América del Sur. Actas Servicio Geológico Minero Argentino, Anales 33, 17−31.

Paul, C.R.C., 2005. Interpreting bioevents: What exactly did happen to planktonic foraminifers across the Cretaceous-Tertiary boundary? Palaeogeography, Palaeoclimatology, Palaeoecology 224, 291−310.

Perch-Nielsen, K., 1981a. New Maastrichtian and Paleocene calcareous nannofossils from Africa, Denmark, the USA and the Atlantic, and some Paleocene lineages. Eclogae Geologicae Helvetiae 73 (3), 831−863.

Perch-Nielsen, K., 1981b. Les nannofossiles calcaires à la limite Crétcé-Tertiaire prés de El Kef, Tunisie. Cahiers Micropaléontologie 3, 25−37.

Perch-Nielsen, K., McKenzie, J., Hé, Q., 1982. Biostratigraphy and isotope stratigraphy and the "catastrophic" extinction of calcareous nannoplankton at the Cretaceous/Tertiary boundary. Geological Society of America Special Paper 190, 353−371.

Pospichal, J.J., 1991. Calcareous nannofossils across the Cretaceous/Tertiary boundary at Site 752, eastern Indian Ocean. Proceedings of the Ocean Drilling Project, Scientific Results 121, 395−414.

Pospichal, J.J., Bralower, T.J., 1992. Calcareous nannofossils across the Cretaceous-Tertiary boundary, Site 761, Nortwest Australian margin. Proceedings of the Ocean Drilling Project, Scientific Results 122, 515−532.

Pospichal, J.J., Wise Jr., S.W., 1990. Calcareous nannofossils across the K/T boundary, ODP Hole 690C, Maud Rise, Weddell Sea. Proceedings of the Ocean Drilling Project, Scientific Results 113, 515−532.

Sass, E., Bein, A., Almogi-Labin, A., 1991. Oxygen-isotope composition of diagenetic calcite in organic-rich rocks: Evidence for $\delta^{18}O$ depletion in marine anaerobic pore water. Geology 18, 839−842.

Scasso, R.A., Concheyro, A., Kiessling, W., Aberhan, M., Hecht, L., Medina, F.A., Tagle, R., 2005. A tsunami deposit at the Cretaceous/Paleogene boundary in the Neuquén Basin of Argentina. Cretaceous Research 26, 283−297.

Schmitz, B., Keller, G., Stenvall, O., 1992. Stable isotope and foraminiferal changes across the Cretaceous-Tertiary boundary at Stevns Klint, Denmark: Argumentsfor long-term oceanic instability before and after bolide impact. Palaeogeography, Palaeoclimatology, Palaeoecology 96, 233−260.

Sissingh, W., 1977. Biostratigraphy of Cretaceous calcareous nannoplankton. Geology Mijnbouw 56, 37−65.

Stinnesbeck, W., Keller, G., 1996. Environmental changes across the Cretaceous-Tertiary Boundary in Northeastern Brazil. In: MacLeod, N., Keller, G. (Eds.), Cretaceous-Tertiary Mass Extinctions: Biotic and Environmental Changes. W.W. Norton & Company, New York, pp. 451−470.

Tantawy, A.A.A., 2003a. Calcareous nannofossil biostratigraphy and paleoecology of the Cretaceous-Tertiary transition in the western desert of Egypt. Marine Micropaloentology 47, 323−356.

Tantawy, A.A.A., 2003b. Maastrichtian calcareous nannofossil biostratigraphy and paleoenvironment of the Mahajanga Basin, Madagascar. Geology of Africa, 3rd Proceedings of the third International Conference on the Geology of Africa, 1, 845−862, Assiut, Egypt.

Tantawy, A.A., Keller, G., 2004. Biotic effects of volcanism on calcareous nannofossils and planktic foraminifera: Ninetyeast Ridge, Indian Ocean. Egyptian Journal of Paleontology 3, 1−23.

Thierstein, H.R., Berger, W., 1979. On Phanerozoic mass extinctions. Naturwissenschaften 66, 46.

Thiry, M., Jacquin, T., 1993. Clay mineral distribution related to rift activity, sea level changes and paleoceanography in the Cretaceous of the Atlantic Ocean. Clay Minerals 28 (1), 61−84.

Twitchett, R.J., 2006. The paleoclimatology, paleoecology and paleoenvironmental analysis of mass extinction events. Palaeogeography, Palaeoclimatology, Palaeoecology 232, 190−213.

Twitchett, R.J., Looy, C.V., Morante, R., Visscher, H., Wignall, P.B., 2001. Rapid and synchronous collapse of marine and terrestrial ecosystems during the end-Permian biotic crisis. Geology 29 (4), 351−354.

Uliana, M.A., Dellapié, D.A., 1981. Estratigrafía y evolución paleoambiental de la sucesión maastrichtiana-eoterciaria del engolfamiento neuquino (Patagonia septentrional). Actas 8° Congreso Geológico Argentino 3, 673−711.

Uliana, M.A., Biddle, K.T., 1988. Mesozoic-Cenozoic paleogeographic and geodynamic evolution of southern South America. Revista Brasileira de Geociencias 18 (2), 172−190.

Varol, O., 1998. Paleogene. In: Bown, P.R. (Ed.), Calcareous Nannofossil Biostratigraphy. Kluwer, Dortrecht, pp. 200−224.

Weaver, C.E., Beck, K.C., 1977. Miocene of SE USA, a model for chemical sedimentation in a peri-marine environment. In: Developments in Sedimentology, vol. 22. Elsevier, Amsterdam, 234 p.

Wei, W., Thierstein, H.R., 1991. Upper Cretaceous and Cenozoic calcareous nannofossils of the Kerguelen Plateau (southern Indian Ocean) and Prydz Bay (East Antarctica). Proceedings of the Ocean Drilling Project, Scientific Results 119, 467−494.

Wignall, P.B., Newton, R., Brookfield, M.E., 2005. Pyrite framboid evidence for oxygen-poor deposition during the Permian-Triassic crisis in Kahsmir. Palaeogeography, Palaeoclimatology, Palaeoecology 216, 183−188.

Wilkin, R.T., Barnes, H.L., Brantley, S.L., 1996. The size distribution of framboidal pyrite in modern sediments: an indicator of redox conditions. Geochimica et Cosmochimica Acta 60 (20), 3897−3912.

Yancey, T.E., 1996. Stratigraphy and depositional environments of the Cretaceous/Tertiary boundary complex and basal section, Brazos River, Texas. Transactions of the Gulf Coast Association of Geological Societies 46, 433−442.

Corrigendum

Corrigendum to: "High stress late Maastrichtian – early Danian palaeoenvironment in the Neuquén Basin, Argentina" [Cretaceous Research 28 (2007) 939–960]

G. Keller [a,*], T. Adatte [b], A.A. Tantawy [c], Z. Berner [d], W. Stinnesbeck [e], D. Stueben [d]

[a] *Department of Geosciences, Princeton University, Princeton, NJ 08540, USA*
[b] *Geological Institute, University of Neuchatel, Neuchatel CH-2007, Switzerland*
[c] *Department of Geology, South Valley University, Aswan, Egypt*
[d] *Institut für Mineralogie und Geochemie, Universität Karlsruhe, 76128 Karlsruhe, Germany*
[e] *Geologisch-Paläontologisches Institut, Universität Heidelberg, Neuenheimer Feld 234, 69120 Heidelberg, Germany*

This paper included among the coauthors Prof. Dr. Héctor A. Leanza of Buenos Aires, Argentina. Dr. Leanza has informed the editor that, although he accompanied coauthor Wolfgang Stinnesbeck to the field in 2002, he did not participate at any stage of the preparation of the manuscript of this paper, nor was he alerted about the submission of the manuscript to Cretaceous Research. His name was introduced in this publication without his knowledge, and he wishes not to be regarded as a coauthor.

The list of authors should therefore read as given above.

* Corresponding author.
E-mail address: gkeller@princeton.edu (G. Keller).